MYELINATED CORTICAL THICKNESS IN BIPOLAR DISORDER

STATISTICAL EXAMINATION OF MYELINATED CORTICAL THICKNESS

IN BIPOLAR DISORDER

By: NADEJDA ZAHARIEVA, B.Sc.

A Thesis Submitted to the School of Graduate Studies in Partial

Fulfillment of the Requirements for the Degree Master of Science

McMaster University MASTER OF SCIENCE (2014) Hamilton, Ontario

(Neuroscience)

TITLE: Statistical Examination of Myelinated Cortical Thickness in

Bipolar Disorder

AUTHOR: Nadejda Zaharieva, B.Sc. (University of Waterloo)

SUPERVISOR: Dr. Nicholas Bock

NUMBER OF PAGES: ix, 50

ABSTRACT

The human cerebral cortex, the outermost layer of the brain, is typically considered in imaging studies to consist of grey matter (GM), with white matter (WM) lying below it. With better imaging techniques, a third tissue type, found between GM and WM, can be identified. This layer contains myelinated axons and is found in the cortex, thus we call it intracortical myelin (ICM), or myelinated grey matter (GMm). We examined the cortical thickness measurements in female patients with bipolar I or II disorders (BD) versus healthy controls. Previous studies have only examined the thickness of the entire cortex, the GM. We developed a processing pipeline and a statistical tool for examining the ICM thickness between two groups. Results show that there are potential differences in GMm between BD and control groups. Further regional and statistical analysis is required to identify the regions of greatest difference, and to confirm significant differences between BD and control groups.

ACKNOWLEDGEMENTS

I'd like to thank my patient supervisor, Dr. Nicholas Bock, for accepting me as a student and being incredibly supportive. I'd also like to thank my former supervisor, Dr. P. Ravi Selvaganapathy, for encouraging me to continue with my graduate studies despite leaving his group.

I'd like to thank the director of neuroscience and committee member of mine, Dr. Kathy Murphy, along with my other committee member and colleague, Dr. Benicio Frey, for their support. I'd also like to thank the neuroscience graduate program coordinator, Sandra Murphy, for encouraging me not to leave the program.

I undoubtedly could not have completed this degree without the support of various health care professionals at McMaster Student Wellness Centre and St. Joseph's Healthcare. I am incredibly thankful for the services and treatments offered! I am also grateful for the various medications – prescription and otherwise – for helping me along the way.

A big thanks to my friend Victor Veitch, for pointing me in the right direction for the statistics portion. Thank you to both my parents for inspiring me with your own graduate degrees.

Finally, and most importantly, a HUGE cuddly thank you to my life partner and best friend, Daniel Sullivan, for being there for me through this difficult time in my life and never losing hope that I could complete this academic and personal challenge. Thank you for helping me out in

any way possible, from making delicious food, to reading boring papers out loud, to telling me I could do it when I was convinced I couldn't.

I am grateful for the experiences I've had over the last two years, the lessons I've learned, and the personal growth that has occurred. I'm grateful to have completed my yoga teacher training during the time I most wanted to drop out of school. I'm grateful for the existence of the ORP Solstice festival in Ontario, and the Ontario Vipassana meditation centre. Finally, I am so grateful that I could work at my own pace, take care of myself, and still finish on time.

I've leveled up, inside and out! Onto the next challenge!

TABLE OF CONTENTS

LIST OF TABLES/FIGURES

CHAPTER 1

LIST OF ABBREVIATIONS AND SYMBOLS

Abbreviation	Definition
α	Significance level
BD	Bipolar disorder
ICM	Intracortical myelin
GM	Grey matter
GMm	Grey matter myelinated
GM-to-GMm	Unmyelinated cortical thickness
GM-to-WM	Total cortical thickness
GMm-to-WM	Myelinated cortical thickness
MRI	Magnetic resonance imaging
SNR	Signal-to-noise ratio
WM	White matter

DECLARATION OF ACADEMIC ACHIEVEMENT

Study design and subject recruitment were carried out by Manpreet Sehmbi under the supervision of Dr. Benicio Frey at St. Joseph's Healthcare Mood Disorders Program and the Women's Health Concerns Clinic in Hamilton, Ontario. MRI data acquisition was carried out by Dr. Benicio Frey and Dr. Nicholas Bock at St. Joseph's Healthcare. Data pre-processing and processing was carried out by Dr. Nicholas Bock at McMaster University.

I, Nadejda Zaharieva was shown all the steps of the pre-processing and processing. I attended an MRI scan of a control subject. I researched statistical analysis using MATLAB's Statistics Toolbox™ and the Statistical Parametric Mapping toolbox (SPM8). I wrote code that can read and write Analyze 7.5 files, as well as calculate several important statistical quantities. I worked with Amira software in order to display and manipulate the images. As far as we know, no available software exists to analyze our images in the manner that we have done.

CHAPTER 1 – INTRODUCTION

The human brain is a fascinating and complex system that has been trying to understand itself for centuries. Only in recent decades has technology allowed us to study the brain in a more detailed and quantifiable manner.

1.1 Cortical Myelin

The brain contains neurons, which transmit information, and glial cells, which provide support to neurons. A type of glial cells known as oligodendrocytes form myelin sheaths around the axons of neurons in the central nervous system (CNS), and this helps increase transmission speed of electrical signals (Kandel et al., 2000). Because of its high lipid content, myelin appears white. The majority of the brain has myelinated axons, and the tissue is referred to as white matter (WM). The thin (2-4mm) outermost layer of the brain is known as the cortex, and it is most commonly referred to as grey matter (GM) because the axons of its neurons are mostly unmyelinated (Kandel et al., 2000).

There do exist however, myelinated fibres within the cortex (Nieuwenhuys, 2013). These fibres are concentrated in radially oriented bundles and tangentially organized layers of varying thickness and compactness throughout the cortex (Nieuwenhuys, 2013). These myelinated areas were discovered over a century ago by Oskar and Cécile Vogt in post-mortem animal and human brains using staining

techniques (Nieuwenhuys, 2013). This gives rise to a third classification of brain tissue we call myelinated grey matter (GMm), which refers to a visible layer of myelin between the WM and the GM within the cortex. We also refer to this as intracortical myelin (ICM). With more recent neuroimaging and processing approaches, we can identify ICM in living human brains (Bock et al., 2009).

1.2 Cortical Thickness and Health

The frontal cortex is primarily associated with cognitive processing, such as thought, language, attention, and perception (Kandel et al., 2000). It is therefore an important part of the brain to consider when examining neurological and psychiatric conditions.

The thinning of grey matter as a whole has been associated with a wide variety of conditions and disorders. Thinning can indicate a number of phenomena: loss of neurons, loss of axons, loss of myelin, or loss of glial cells. Thinning of the cerebral cortex has been found in neurological disorders such as Huntington's disease (Rosas et al., 2002), multiple sclerosis (Sailer et al., 2003), Alzheimer's disease (Querbes et al., 2009), and Parkinson's disease (Pereira et al., 2012), as well as psychiatric disorders such as attention deficit hyperactivity disorder (Makris et al., 2007), schizophrenia (Narr et al., 2005), major depressive disorder (Truong et al., 2013), and bipolar disorder (Lyoo et al., 2006). It is also

important to note that the cortex tends to thin with normal aging as well (Hutton et al., 2009).

More recently, the ICM, or myelinated grey matter layers, have been specifically examined in schizophrenia (Bartzokis et al., 2009). It was found that the frontal ICM volume was lower in patients versus controls, and varied between medications (Bartzokis et al., 2009).

Examining the ICM layers is an entirely new area of study not previously possible due to historical lower resolution and contrast in brain images. It is therefore of high interest that myelinated grey matter be examined in other conditions. In this project, we are studying patients with bipolar disorder and healthy controls.

1.3 Bipolar Disorders

Bipolar disorders (BD) affect 1.5-3.0% of the general population (Strakowski et al., 2004). The DSM-IV-TR divides bipolar spectrum disorders into three main categories (American Psychiatric Association, 2000):

1. Bipolar 1 Disorder, in which there is cycling between episodes of mania and depression.

2. Bipolar 2 Disorder, in which there is cycling between episodes of hypomania (a milder state of mania) and depression.

3. Cyclothymic Disorder, in which there is cycling between episodes of hypomania and depression that do not reach the full diagnostic standard for hypomanic or depressive episodes.

A manic episode is characterized by "a distinct period of abnormally and persistently elevated, expansive, or irritable mood, lasting at least 1 week (or any duration if hospitalization is necessary)" (DSM-IV-TR, 2000). A hypomanic episode is characterized by "a milder state of mania in which the symptoms are not severe enough to cause marked impairment in social or occupational functioning or need for hospitalization, but are sufficient to be observable by others" (DSM-IV-TR, 2000). A depressive episode is characterized by "depressed mood and/or loss of interest or pleasure in life activities for at least 2 weeks and [...] symptoms that cause clinically significant impairment in social, work, or other important areas of functioning almost every day" (DSM-IV-TR, 2000).

In this study, we examine patients with bipolar I or II disorder and healthy controls.

1.4 Magnetic Resonance Imaging of Myelin

Magnetic resonance imaging (MRI) is a medical imaging technique which produces 3D images of the anatomy and structure of the organ scanned, in this case the brain. Unlike other brain imaging techniques, MRI does not use ionizing radiation, and is therefore safer.

The principle of an MRI scanner relies on the idea that the hydrogen atoms within the human body are magnetically active (McRobbie, 2007). The MRI has three types of magnetic fields, a strong constant field, B_0, spatially varying gradient fields, B_x, B_y and B_z, and an oscillating radio frequency (RF) field, B_{rf} (McRobbie, 2007). The gradient fields vary slightly in strength along the x, y, and z axes in order to encode for location. With the constant field B_0 on, the hydrogen nuclei align parallel or anti-parallel to its direction, and precess like spinning tops at a frequency specific to hydrogen and related to the B_0 strength (Callaghan, 1991). When the RF field is turned on briefly, the hydrogen nuclei tilt away from B_0, and then return when it's turned off. This return is called "relaxation", and the nuclei release some energy, which is then recorded by detectors (McRobbie, 2007).

The relaxation time can be divided into two components: T_1, the longitudinal relaxation time, and T_2, the transverse relaxation time. Because different tissues have different relaxation times, they appear brighter or duller in T_1 or T_2-weighted images (Callaghan, 1991). This represents the primary contrast mechanism in neuroimaging with MRI, because gray and white matter have different T_1's and T_2's. In this study, we used optimized T_1-weighted imaging to obtain the highest contrast between WM and GMm (Bock et al., 2013).

1.5 Cortical Thickness Measures

The brain has previously been divided into two tissue types, GM and WM, according to the intensity values in MRI images (Kapur et al., 1996). Here, we will divide the brain into three tissue types: GM, WM, and GMm. We define the distances between the boundaries as: GM-to-WM, total cortical thickness; GM-to-GMm, unmyelinated cortical thickness; and GMm-to-WM, myelinated cortical thickness. Figure 1 illustrates these boundaries and distances.
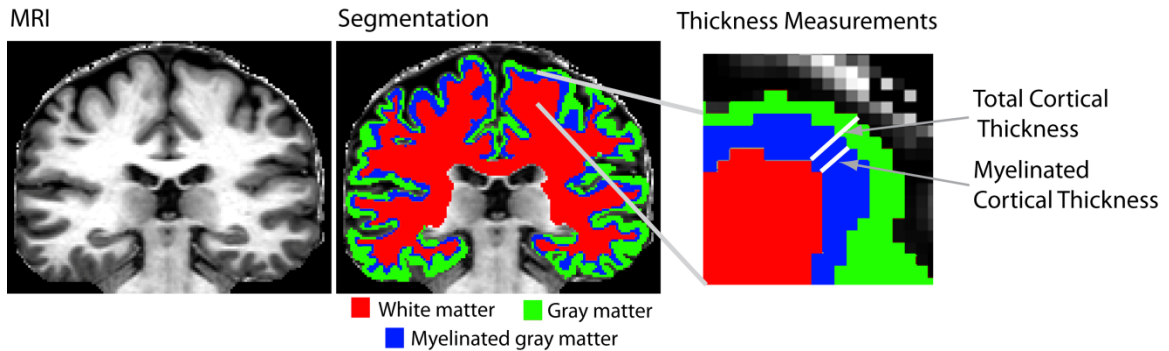

Figure 1 – Segmented cortical boundaries.
(Hashim et al., *Second annual Whistler scientific workshop on brain functional organization, connectivity, and behaviour*, 2014).

1.6 Hypothesis

Our big question is ultimately whether any of these three thicknesses are statistically different between BD patients and healthy controls. Specifically, we would like to investigate changes in the thickness of the ICM layers in the frontal lobe, as this could represent a loss or gain of myelin, indicating disrupted circuits in BD. While our study currently contains only a limited number of subjects in control and BD groups, the purpose of this thesis is to develop a statistical

framework for investigating these changes in future studies with larger cohorts of subjects.

We begin by taking an average of each group and comparing each corresponding data point, or voxel, between the average images. The three null hypotheses are: For every point on the surface of the brain in the MRI image, there is no difference in (1) myelinated, (2) unmyelinated, (3) total cortical thickness between BD and control brains.

CHAPTER 2 – METHODS

We worked in conjunction with St. Joseph's Healthcare in Hamilton to obtain and analyze MRI data of BD and control subjects. Data processing took place at McMaster University.

2.1 Subject Recruitment

Subjects were recruited through the Mood Disorders Program & Women's Health Concerns Clinic at St. Joseph's Healthcare in Hamilton, Ontario (Frey et al.) as part of a project on blood markers. Experiments were approved by the Research Ethics Board at St. Joseph's Healthcare, and informed consent was obtained from each subject. 10 female BD patients and 10 female age-matched controls were recruited. "Inclusion criteria for both groups was: Age 18-45, right-handed, premenopausal, regular menstrual cycles, and no use of hormonal agents. Inclusion criteria for BD subjects: Diagnosis of BD type-I or type-II according to the SCID-I, and being euthymic for at least 3 months. Exclusion criteria: Any current co-morbid Axis I psychiatric diagnosis (for BD subjects), alcohol/substance abuse within the past year (excluding caffeine and nicotine), past or current history of neurological disorders including head trauma and migraines, unstable general medical conditions and presence of any contra-indications for MRI" (Frey et al.).

Out of the 20 total scans, 2 BD and 2 control scans were excluded due to artifacts in the images, either due to motion during the scan, or

incorrect imaging procedure. The final dataset contains $N_1=8$ control and $N_2=8$ bipolar. Table 1 summarizes the demographics of the final 16 subjects.

Control	Age	Bipolar	Age
Subject 1	22	Subject 1	29
Subject 2	23	Subject 2	36
Subject 3	23	Subject 3	41
Subject 4	45	Subject 4	32
Subject 5	26	Subject 5	42
Subject 6	44	Subject 6	28
Subject 7	41	Subject 7	42
Subject 8	47	Subject 8	42
Mean	33.9	Mean	36.5

Table 1 – Subject demographics.

2.2 MRI Data Acquisition

The MRI scanner used was a 3.0 Tesla General Electric whole body short bore scanner (Software Version 22.0) with a 32-channel receive-only coil for the head (MR Instruments) and a transmit body coil (GE). Subjects were scanned during the follicular phase of the menstrual cycle (Frey et al.). Blood samples were collected on the same day as the scan in order to be correlated with white matter content (Frey et al.).

Three types of images were collected: an Anatomical Reference image, the T_1-weighted image, and a Ratio image. Each of these images

were 3D and had a 1mm isotropic resolution. A description of the sequences used is found below:

Anatomical Reference image: A reference image, made using a 3D inversion-recovery gradient echo sequence (GE 3D BRAVO) with the parameters: Inversion time = 450 ms, TE = 3.2 ms, TR in acquisition block = 8.4 ms, flip angle in acquisition block = 12°, FOV = 25.6 x 25.6 x 25.6 cm, matrix = 256 x 256 x 256, linear phase encoding, Autocalibrating Reconstruction for Cartesian imaging (ARC) parallel imaging factor of 2 in the second phase encode direction, Number of averages = 1, time = 5 min 32 s.

T_1-weighted image: An image with increased intracortical contrast, made using four separate images collected with an inversion-recovery gradient echo sequence (GE 3D BRAVO) with the parameters: Inversion time = 1100 ms, Time between end of acquisition block and next 180° pulse (TD) = 1000 ms TE = 3.2 ms, TR in acquisition block = 8.4 ms, flip angle in acquisition block = 12°, FOV = 24.0 x 10 (selective slab in left/right direction) x 24.0 cm, matrix = 240 x 100 x 240, centric phase encoding, ARC factor 2 in second phase-encoding direction, Number of averages = 1, time = 5 min 53 s. To increase intracortical contrast, each hemisphere was imaged separately. To increase SNR, each hemisphere was imaged twice. Each of the four separate images were registered to the anatomical reference image using a 6-parameter affine

transformation (FLIRT Tool in FSL Version 5.0 (fsl.fmrib.ox.ac.uk/fsl/))
(Jenkinson et al., 2012). The images were then summed to create the
final image of the whole head.

Ratio image: An image that corrects B_1 inhomogeneity artifacts in
the T_1-weighted image, made with a 3D gradient-echo sequence (GE 3D
SPGR) with the parameters: TE = 3.1 ms, TR = 7.9 ms, flip angle = 4°,
FOV = 24.0 x 17.4 x 24.0 cm, matrix = 240 x 174 x 240, Number of
averages = 1, time = 5 min 29 s. The proton-density weighted image was
registered to the T_1-weighted image using a 6-parameter affine transform
(FSL). It was then filtered with a 3D median filter with a 5 x 5 x 5 kernel
size. Finally, the T_1-weighted image was then divided by the filtered
proton-density weighted image to create the ratio image.

2.3 Data Processing

Image processing was performed predominantly in MIPAV v7.0.1
software (mipav.cit.nih.gov) using the CBS High-Res Brain Processing
Tools Version 3.0 plug-ins (www.nitrc.org/projects/cbs-tools/). The
following procedure was performed:

1. Generate labels identifying the cerebrum. Use the SPECTRE 2010
   algorithm (Carass et al., 2011) on the T_1-weighted image to remove
   the skull.
2. Use the Multiple Object Geometric Deformable Model (MGDM)
   Multi-contrast Brain Segmentation algorithm (Bogovic et al., 2013)

on the Ratio image to generate probabilistic labels for tissue classes in the brain.

3. Use the CRUISE algorithm (Landman et al., 2013) on the probability labels to generate smoothed, topologically correct labels for the cerebrum.

4. Manually inspect and correct the labels.

5. Remove subcortical structures (as identified by the MGDM algorithm) from the labels and mask the Ratio image.

6. Use the Fantasm algorithm (Pham, 2001) to segment the masked Ratio image into the three tissue classes (GM, GMm, WM) based on a fuzzy c-means clustering algorithm. Binary labels for GM and GMm are taken at a fuzzy threshold of 1. The labels for WM are taken at a fuzzy threshold of 0.1 and then morphologically processed.

7. Smooth the GMm labels in Amira 5.2.2 (www.vsg3d.com/amira/) using 3D morphological smoothing with a kernel size of 2.

8. Remove GMm identified in the outermost layers of the cortex.

9. Calculate the levelsets, φ, using the Distance Field algorithm (Sethian, 1999).

10. Calculate the distances between boundaries. The distances for individual subjects are visualized on the pial surface in Amira.

11. Register the images for each individual to the ICBM 152 atlas space (Fonov et al., 2011; Fonov et al., 2009) using FSL Version 5.0 (Jenkinson et al., 2012) using the parameters in the T1_2_MNI152_2mm.cnf file.

12. Apply the warp to each distance file.

13. Visualize the distance images in Amira using a surface mesh created from the pial surface of the ICBM 152 atlas.

Because each brain has a unique size, shape, and folding, they are mapped – or registered – to the same space (ICBM 152), so we may compare each voxel location meaningfully.

Each image is 182 × 218 × 182 voxels = 7 221 032 total. When mapped onto the brain surface, the relevant data falls onto 578 194 points on the pial surface (286 246 right hemisphere, 291 948 left hemisphere). It can thus be said that we have 578 194 thickness measurements in each thickness map of the brain.

2.4 Statistical Analysis

The statistical analysis of MRI data is not a trivial matter. One of the most common types of statistical test used is the Student's t-test. T-tests assume normally distributed data. This assumption may not always hold true for measures in the human brain such as cortical thickness, but is a reasonably good approximation.

When comparing two groups, as we are here with BD and control, a two-sample t-test is used, as opposed to a one-sample test. Because our groups are comparing different individuals (as opposed to, for example, the same group before and after a treatment), an unpaired t-test is used. In this parametric test, we assume that the variance within the control population is equal to the variance within the BD population. We also assume that both datasets are normally distributed.

The result of the t-test is proportional to the difference between the two sample means, and inversely proportional to their variances. The t-statistic can be converted to a p-value between 0 and 1, with a value closer to 0 being more significant. This value can be conceptually thought of as a probability of the difference being significant. For example, if we obtain p = 0.001, the probability of there being a statistically significant difference is (1–p)×100% = (1–0.001)×100% = 99.9%.

This would normally be straight forward, except that we are not comparing only one voxel in the brain. The number of voxels on the surface of the cortex that we are interested in is 578 194, and in our analysis we are comparing all 7 221 032 voxels because it is not trivial to separate those which contain our data of interest from those which do not. In any case, we are doing hundreds of thousands of t-tests, or comparisons. With each comparison, we increase our chance of a false

positive, or Type I error, which means we may fail to reject the null hypothesis when we should be (Lindquist, 2008). Another way of looking at it, is if we choose a confidence level, $1-\alpha$, of 0.05 for example, then we can only be confident about $(1-\alpha)\times100\%$ or 95% of our results, and 5% of them could be false positives but we would not know it.

There are numerous ways of taking into account multiple comparisons such as the ones made in MRI analysis (Genovese et al., 2002). A common solution is to use a multiple comparisons correction, such as the Bonferroni correction. Here, the significance α is simply divided by the number of comparisons being made (Genovese et al., 2002). In our case, if we want to use $\alpha=0.05$, in other words, we want to be 95% confident, we would divide α by 578 194 to yield $\alpha= 8.65\times10^{-8}$. This means that our p-value has to be below 8.65×10^{-8} in order to be 95% certain it is significant. Clearly, the Bonferroni correction is much too conservative in protecting from false positives, and we end up with many false negatives, or Type II errors (Genovese et al., 2002).

Many MRI studies use the Bonferroni correction or other multiple comparison corrections, but most divide the brain up into regions of interest, or ROI's (Thompson et al., 2001; Makris et al., 2007; Sailer et al., 2003; Sowell et al., 2003). When taking into account an ROI, one only has to divide the significance α by the number of voxels in that ROI, yielding slightly less conservative p-values. In the extreme, all thickness

values in the ROI can be summed into a single measure, which will also greatly increase statistical power. The ability to localize changes at a fine resolution in the brain is lost, however.

Another solution to the Bonferroni problem is to use an expected false discovery rate (FDR) in order to choose a better p-value threshold (Genovese et al., 2002). Some studies choose to use this method (Schwartzman et al., 2009; Shaw et al., 2006; Rimol et al., 2010). This also requires using only the relevant data points, which we have not separated from the entire brain as of yet.

Other methods for working around the multiple comparisons problem include using principal component analysis (PCA) (Narr et al., 2005), random field theory (RFT) (Truong et al., 2013), and resampling, which includes jackknifing, bootstrapping, and permutation tests (Thompson et al., 2005; Foland-Ross et al., 2011). It is very common in neuroimaging to simply use a lower α threshold such as 0.001 to approximate a multiple comparison correction (Lyoo et al., 2006; Rosas et al., 2002; Pereira et al., 2012; Querbes et al., 2009), often in combination with ROI analysis.

We chose to use an uncorrected α=0.05 and α=0.001, and a Bonferroni corrected α=0.05 in our analysis. 0.05 is a common threshold in preliminary analysis, and 0.001 is used as a less strict approximation of the Bonferroni correction (Lyoo et al., 2006). All calculations were

preformed in MATLAB R2013a (8.1)

(http://www.mathworks.com/downloads/web_downloads/), using the

Statistics Toolbox™ (8.2) and the Image Processing Toolbox (8.2). Table 2

outlines the statistical tests we included in our analysis.

Quantity	Explanation	MATLAB Function
Means	-	mean
Standard deviations	-	std
Coefficients of variation	standard deviation/mean	-
Difference of the means	mean1 – mean2	-
Percent difference	(mean1 – mean2)/mean1 × 100%	-
T-statistics	-	ttest2
P-values	-	ttest2
Significance	1 (significant) or 0 (not significant)	ttest2

Table 2 – Statistics included in analysis.

The code outputs results into Analyze 7.5 format images (*.img

extension with *.hdr header file), which can then be viewed and analyzed

with most imaging software such as Amira.

CHAPTER 3 – Results

Results of our calculations were displayed in Amira imaging software, and screenshots were obtained. Results are summarized visually in Figures 2-28.

Some minor errors in the processing stages remain uncorrected. A comparison of one correct and one incorrect brain image is provided in Figures 2, 11, and 20. The difference won't significantly affect statistical analysis.

In the rainbow legend, the bluer areas are thinner and the redder areas are thicker. In the blue/grey/red legend, the blue areas represent thicker areas in BD and the red areas represent thicker areas in controls. In the hypothesis tests, blue represents "statistically insignificant" and red represents "statistically significant".

3.1 Myelinated Cortical Thickness

This is the thickness measure of most interest to this study. Figures 3 and 4 show the individual brains of control and bipolar subjects after registration, respectively. Figures 5-7 show the means, standard deviations, and coefficients of variation, respectively. Figure 8 shows the difference of the means and the percent difference. Figure 9 shows the results of the t-test and the p-values. Figure 10 shows the areas of statistical significance.
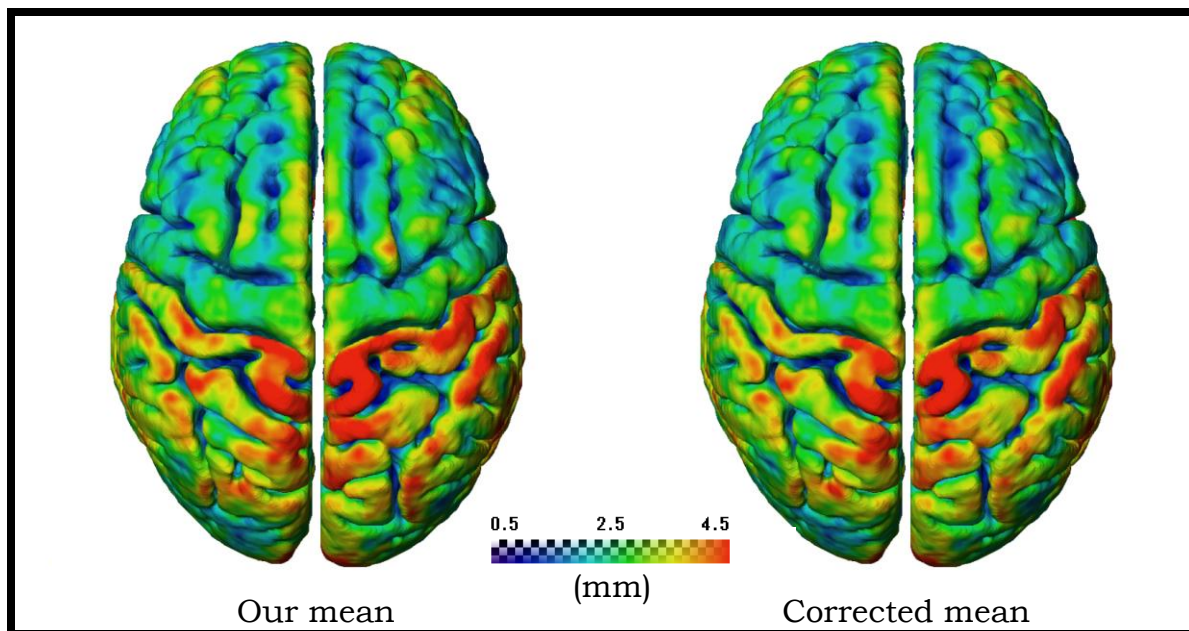
Figure 2 – GMm-to-WM mean versus correct mean of controls.
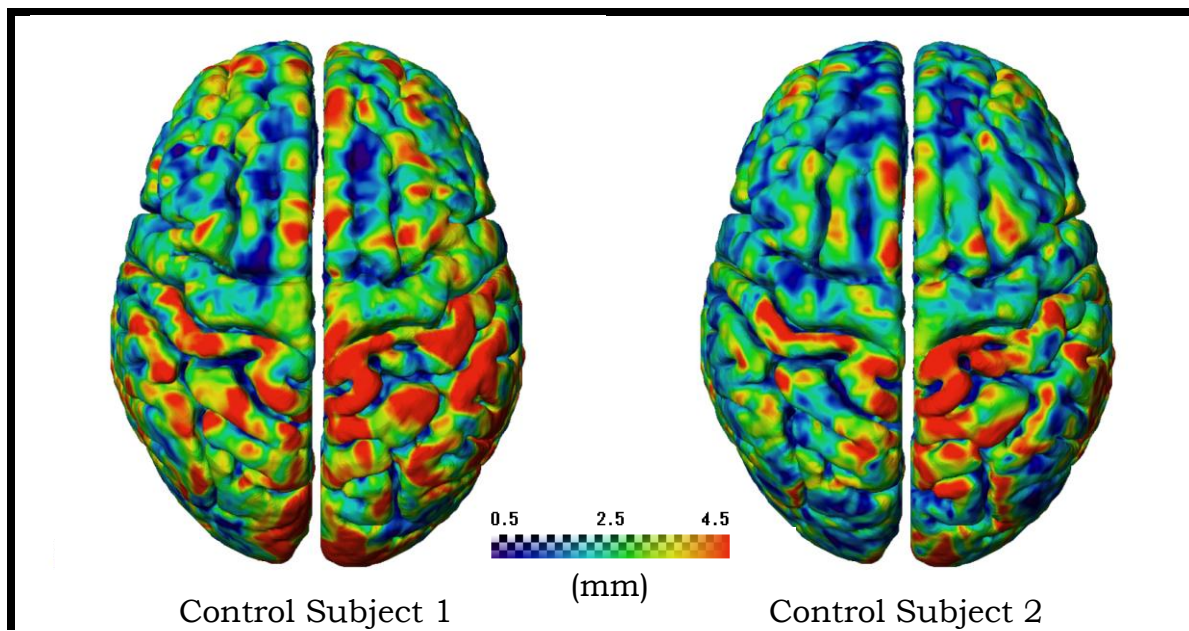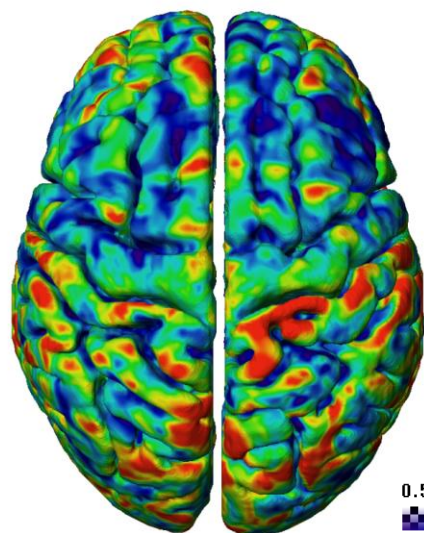
Control Subject 3

Control Subject 4
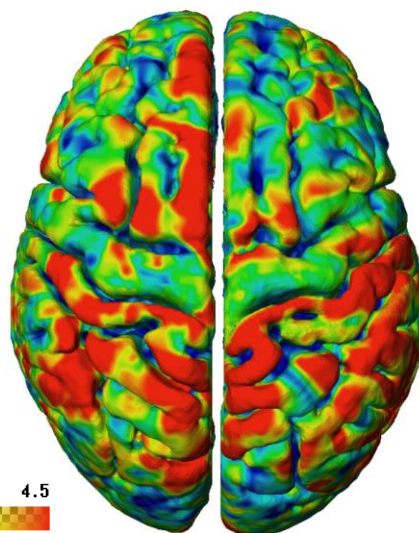
Control Subject 5
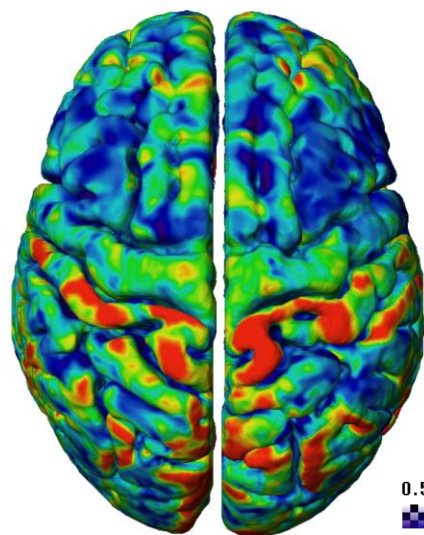
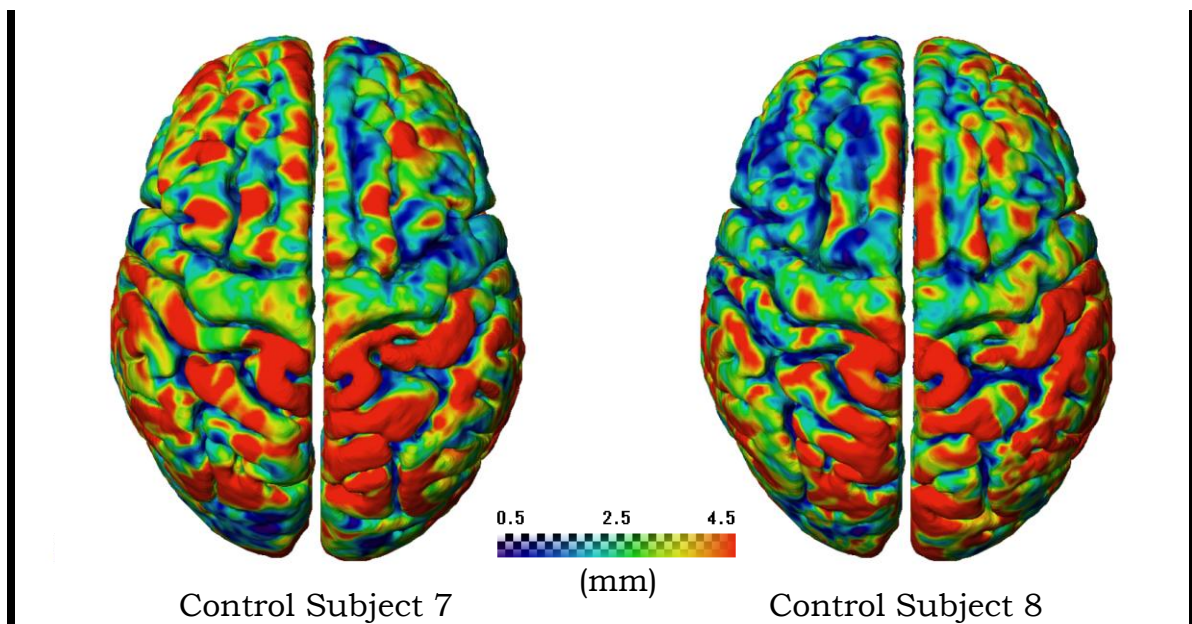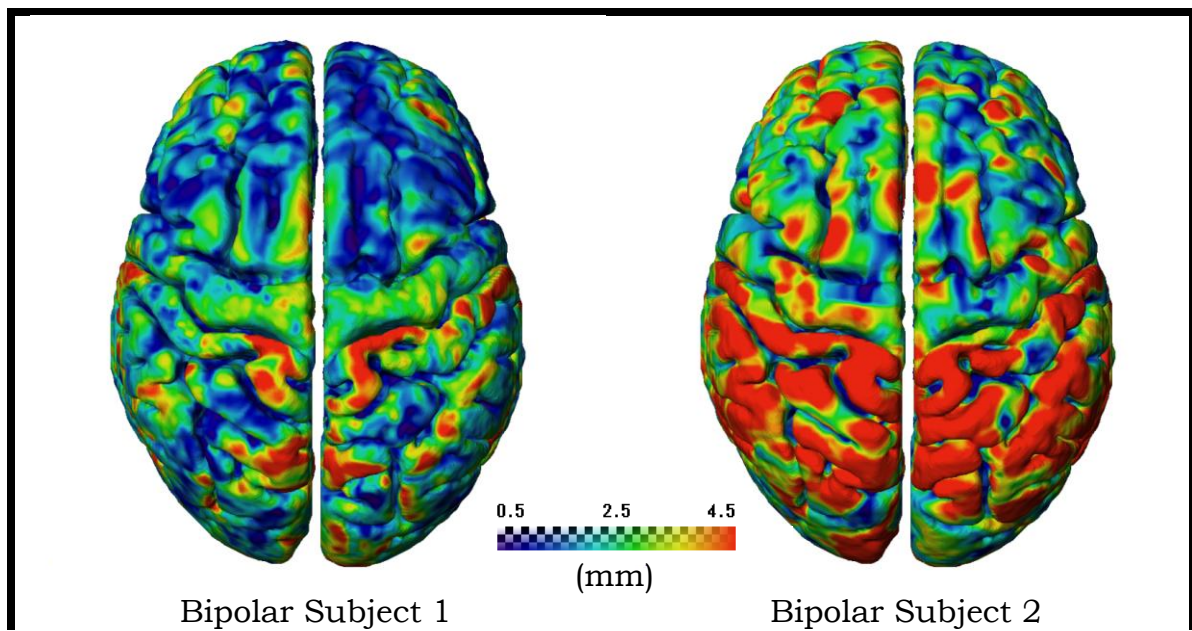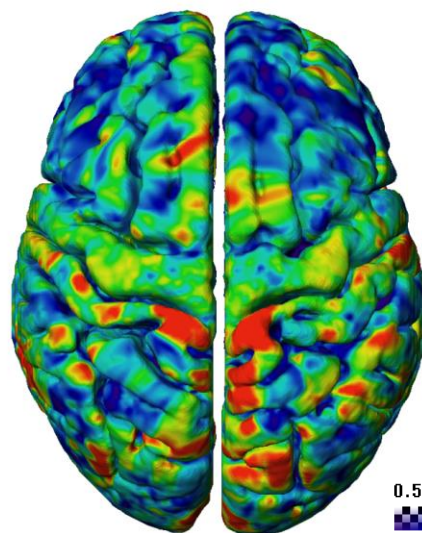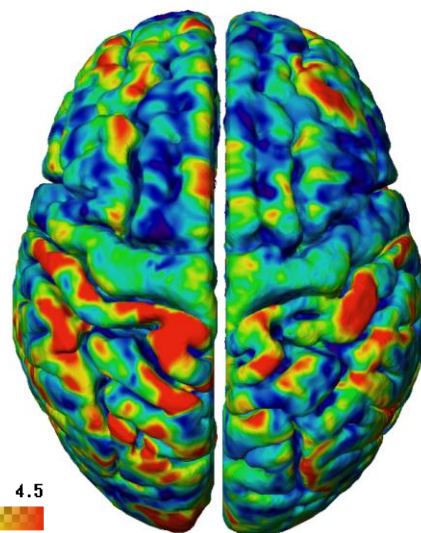Control Subject 6
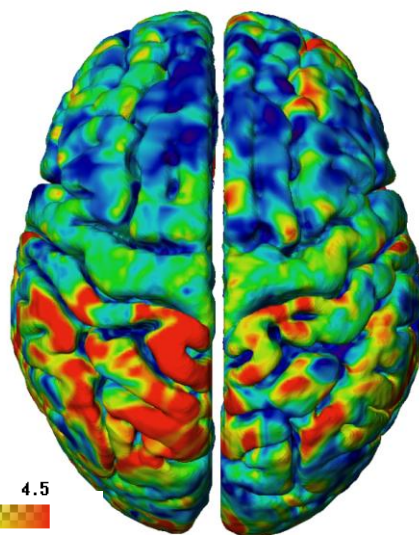
Control Subject 7 — Control Subject 8

Figure 3 – GMm-to-WM of individuals in control group.
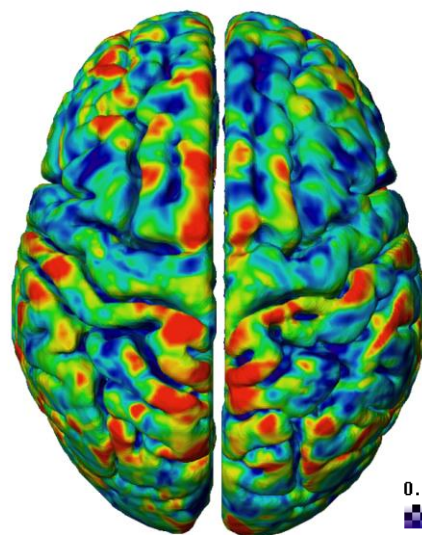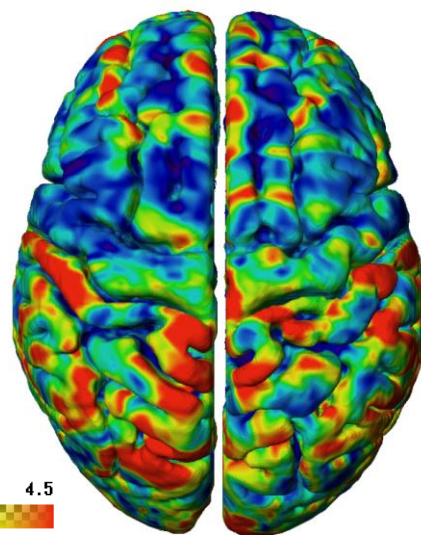

Bipolar Subject 1 — Bipolar Subject 2

Bipolar Subject 3

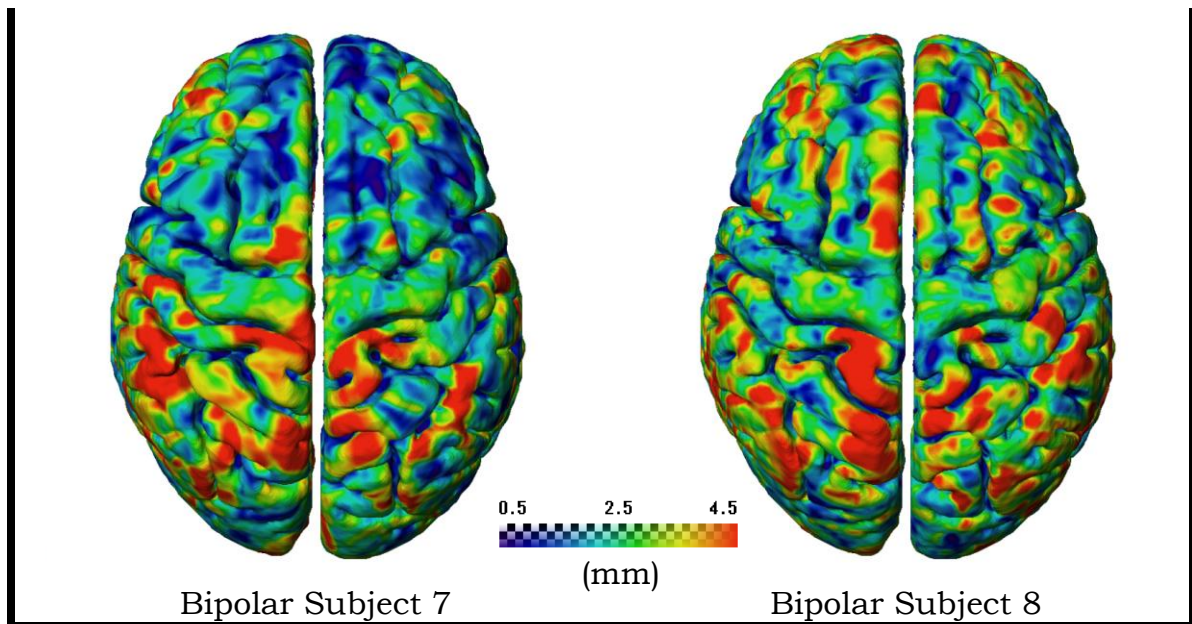Bipolar Subject 4

Bipolar Subject 5

Bipolar Subject 6
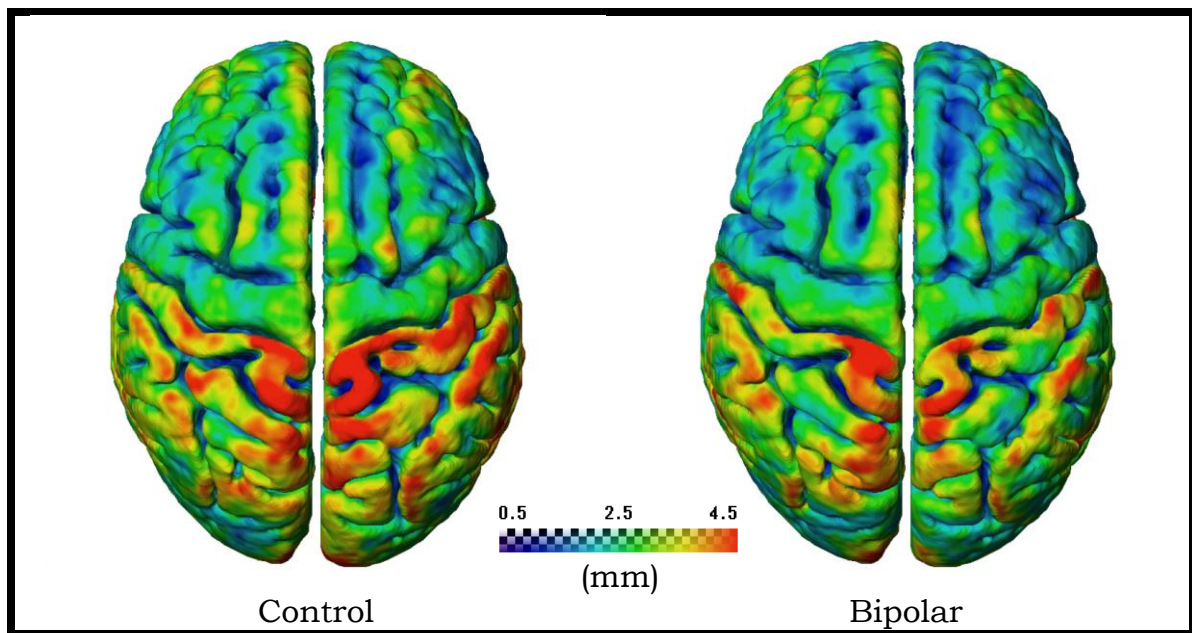
Figure 4 – GMm-to-WM of individuals in bipolar group.

Figure 5 – Mean of GMm-to-WM.

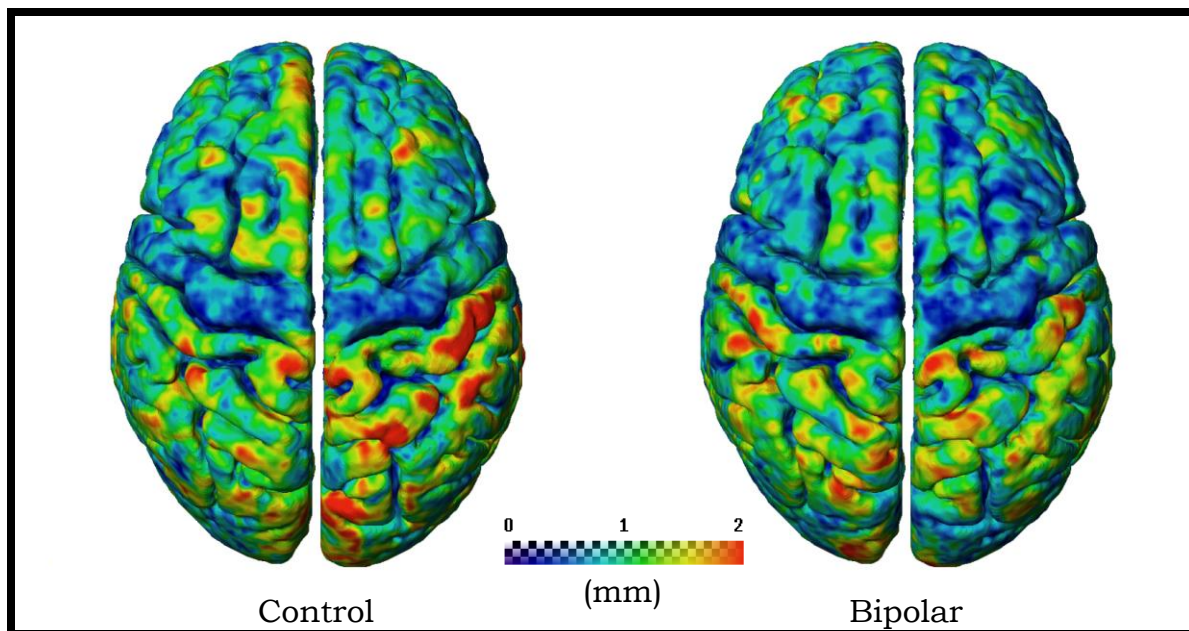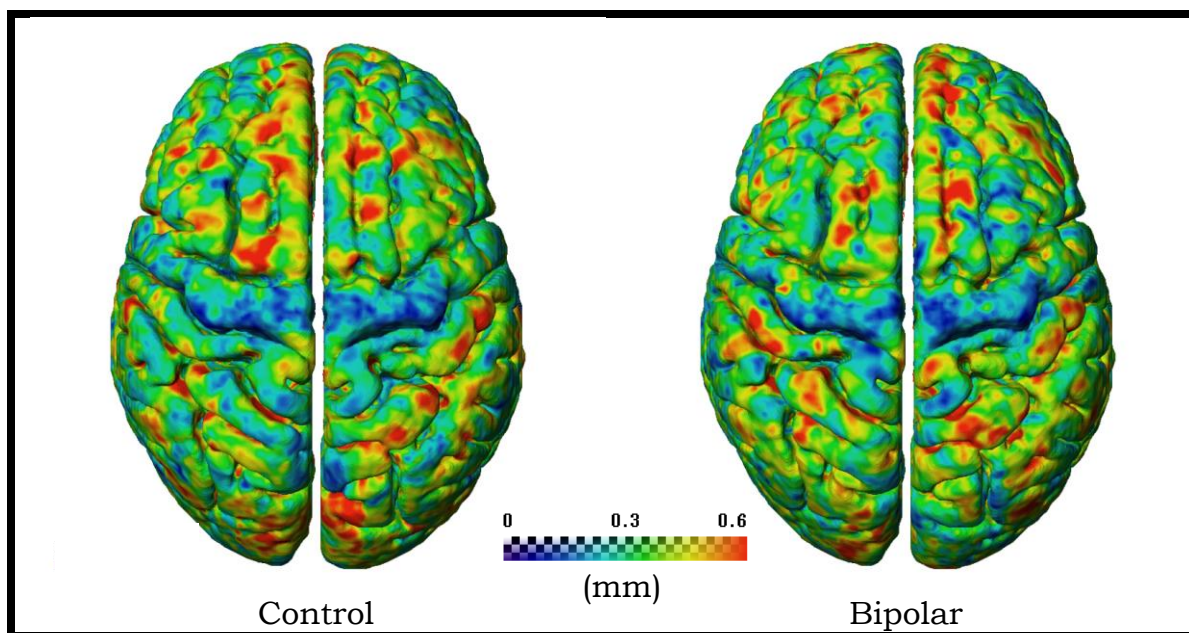Figure 6 – Standard deviation of GMm-to-WM.
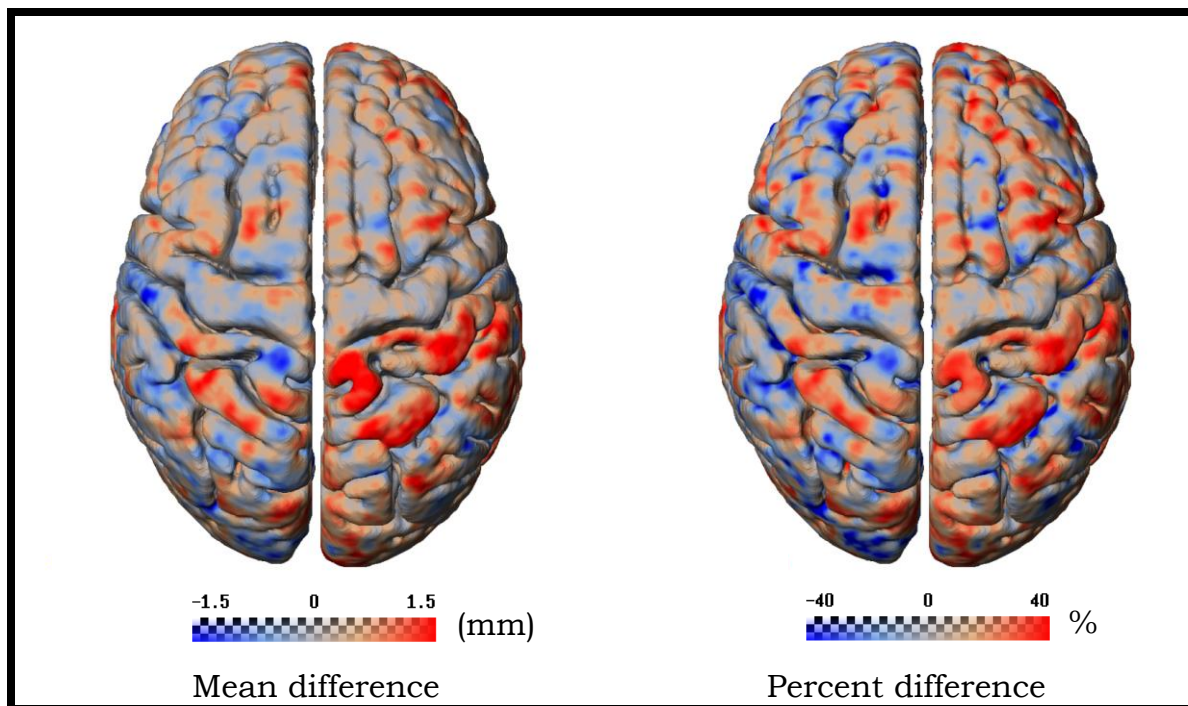

Figure 7 – Coefficient of variation of GMm-to-WM.

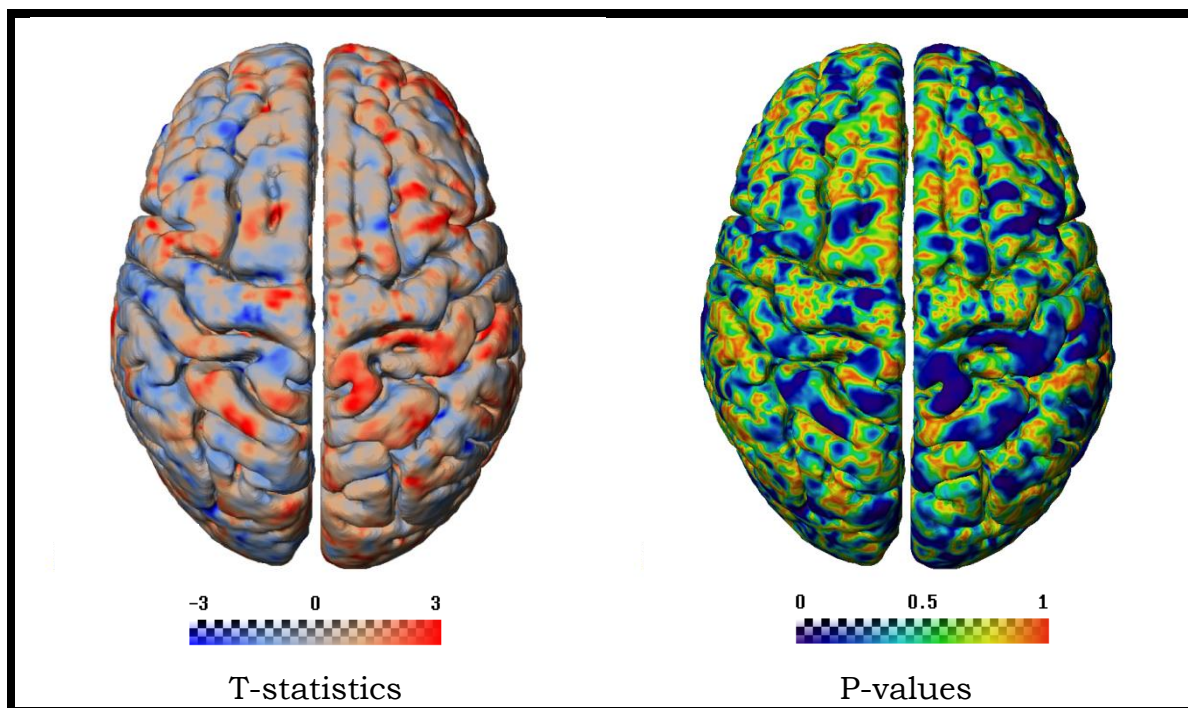Figure 8 – Mean difference and percent difference of GMm-to-WM.

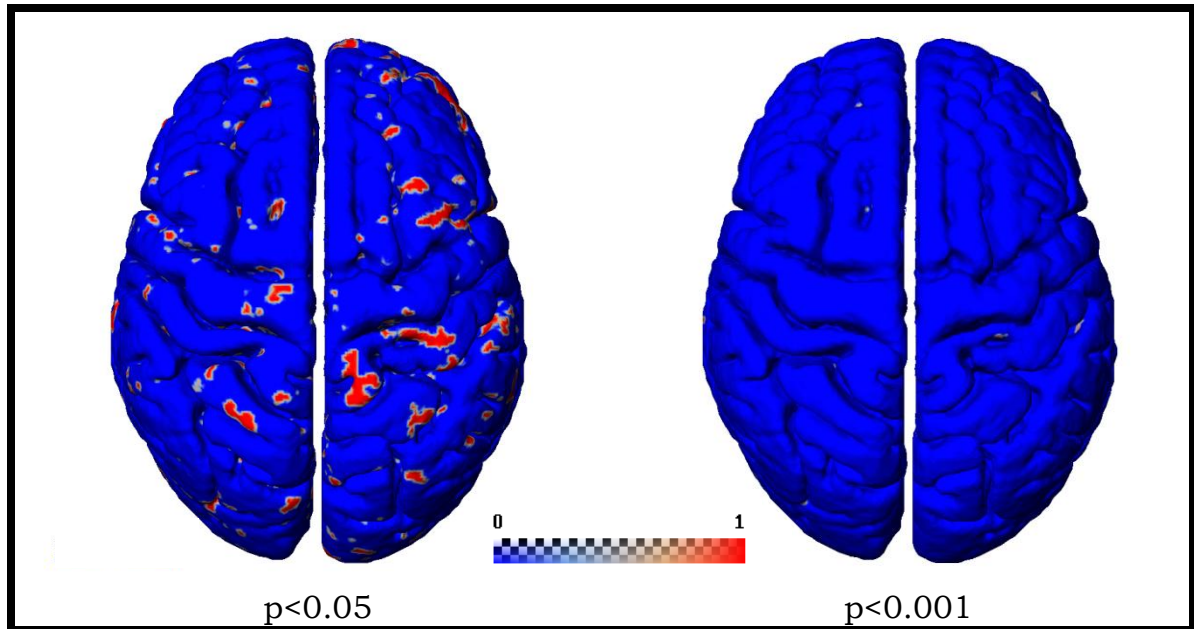Figure 9 – T-statistics and p-values of GMm-to-WM.

p<0.05   p<0.001

Figure 10 – Significances of GMm-to-WM.

3.2 Unmyelinated Cortical Thickness

Figures 12 and 13 show the individual brains of control and bipolar subjects after registration, respectively. Figures 14, 15, and 16 show the means, standard deviations, and coefficients of variation, respectively. Figure 17 shows the difference of the means and the percent difference. Figure 18 shows the results of the t-test and the p-values. Figure 19 shows the areas of statistical significance.
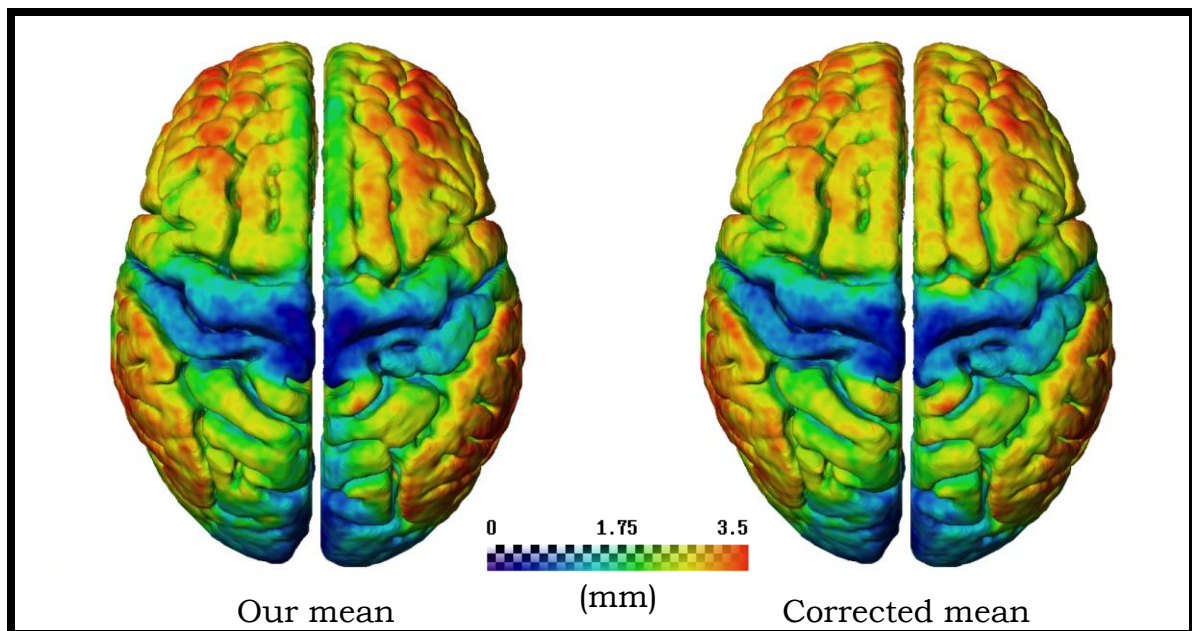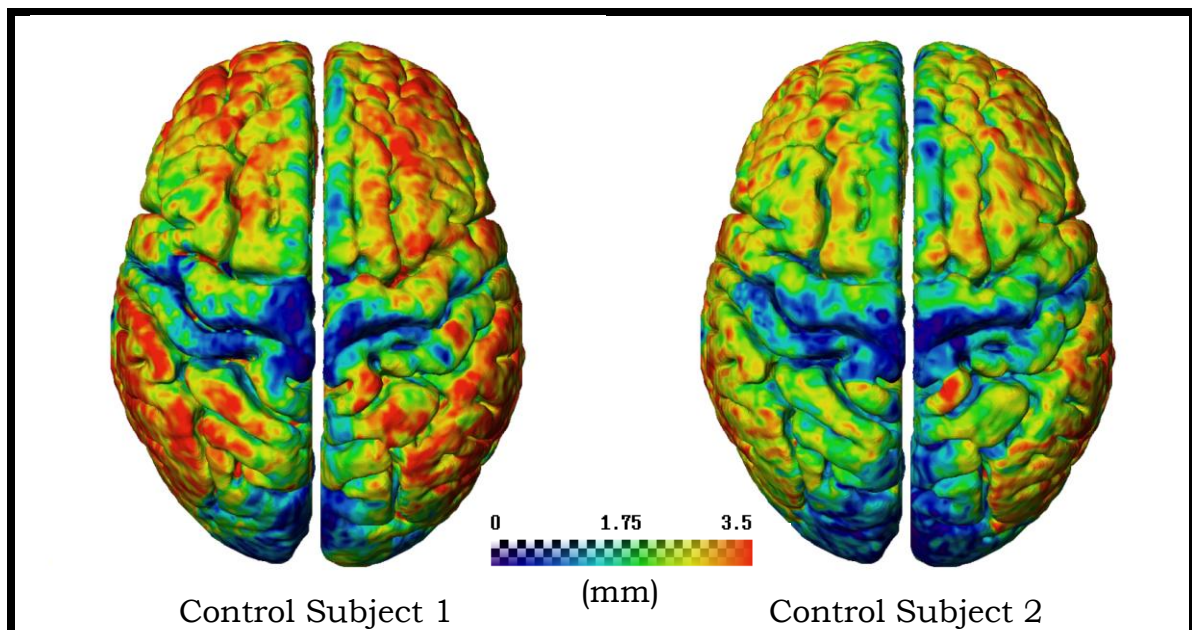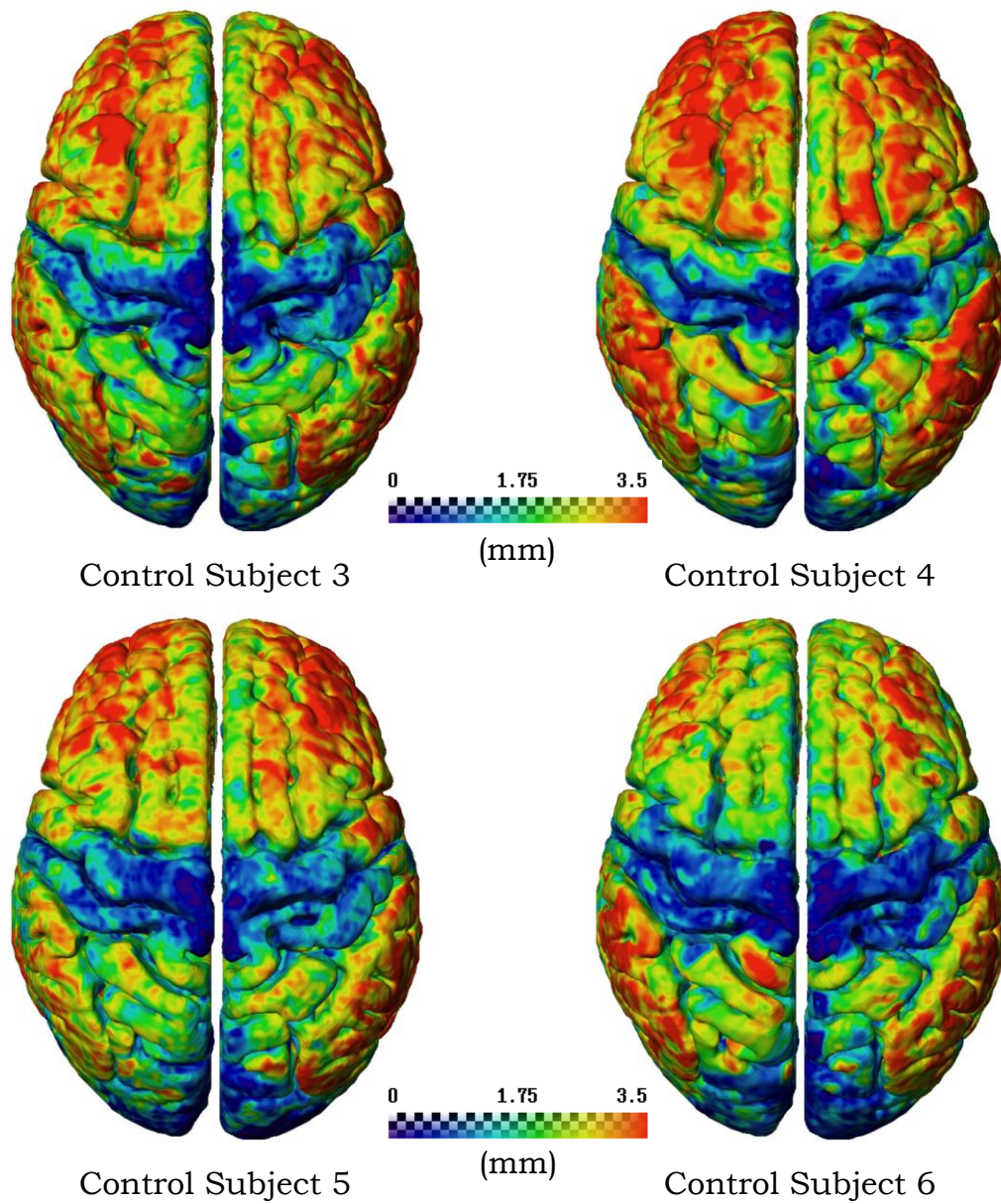
Figure 11 – GM-to-GMm mean versus correct mean of controls.

Control Subject 3

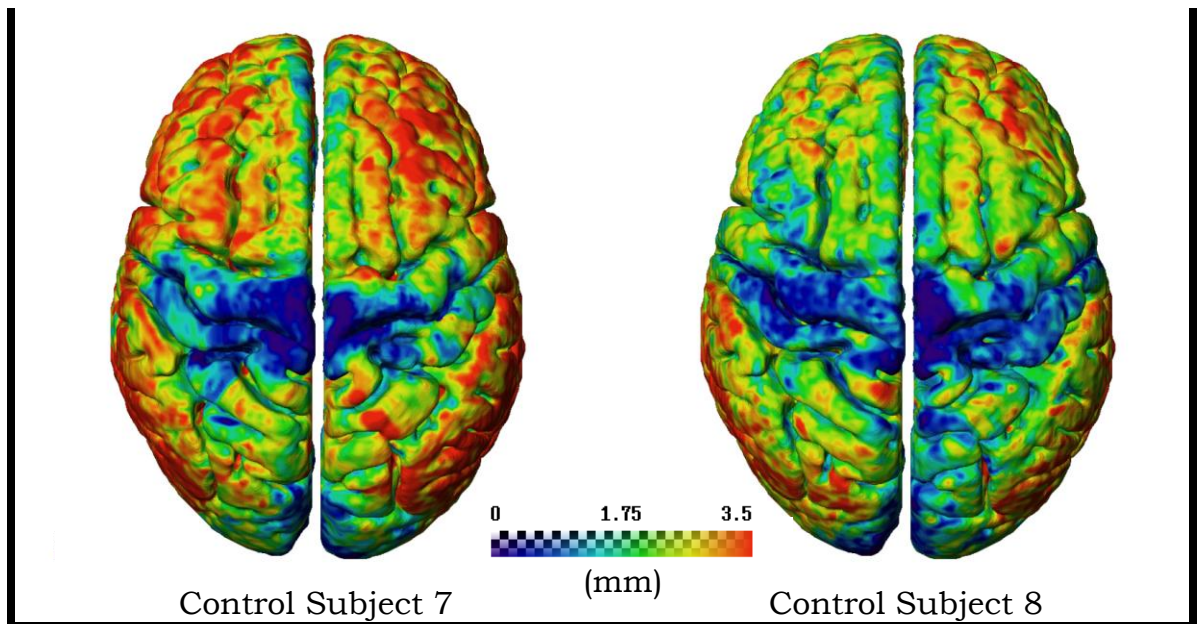Control Subject 4

Control Subject 5

Control Subject 6

Control Subject 7   (mm)   Control Subject 8

Figure 12 – GM-to-GMm of individuals in control group.

Bipolar Subject 1   (mm)   Bipolar Subject 2

Bipolar Subject 3

(mm)

Bipolar Subject 4

Bipolar Subject 5

(mm)

Bipolar Subject 6
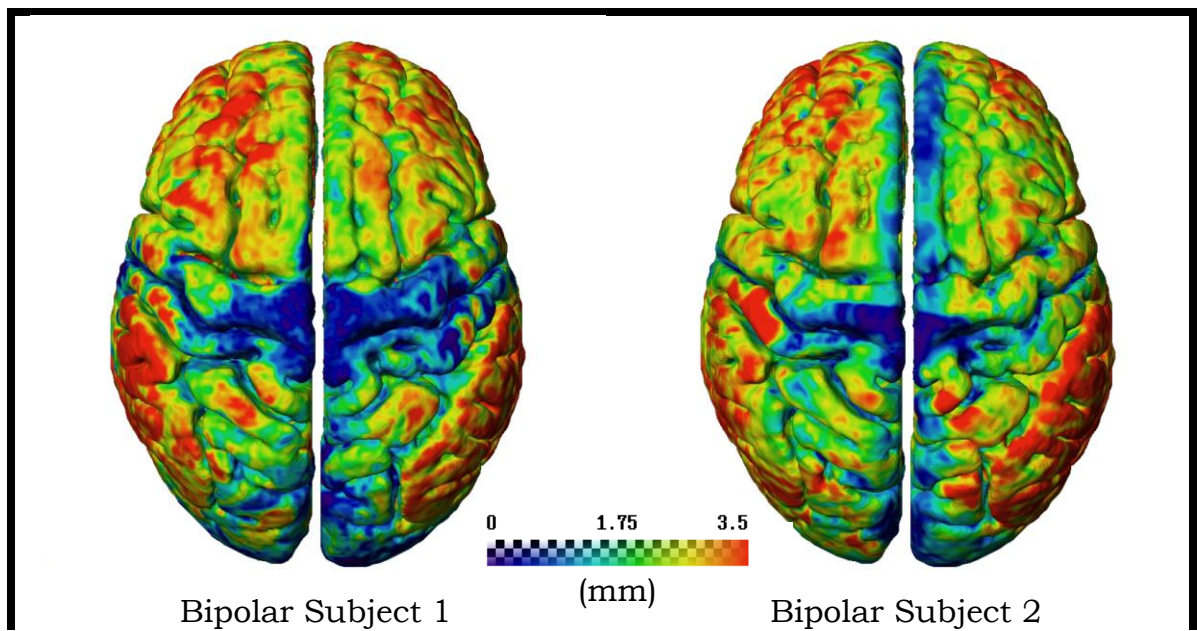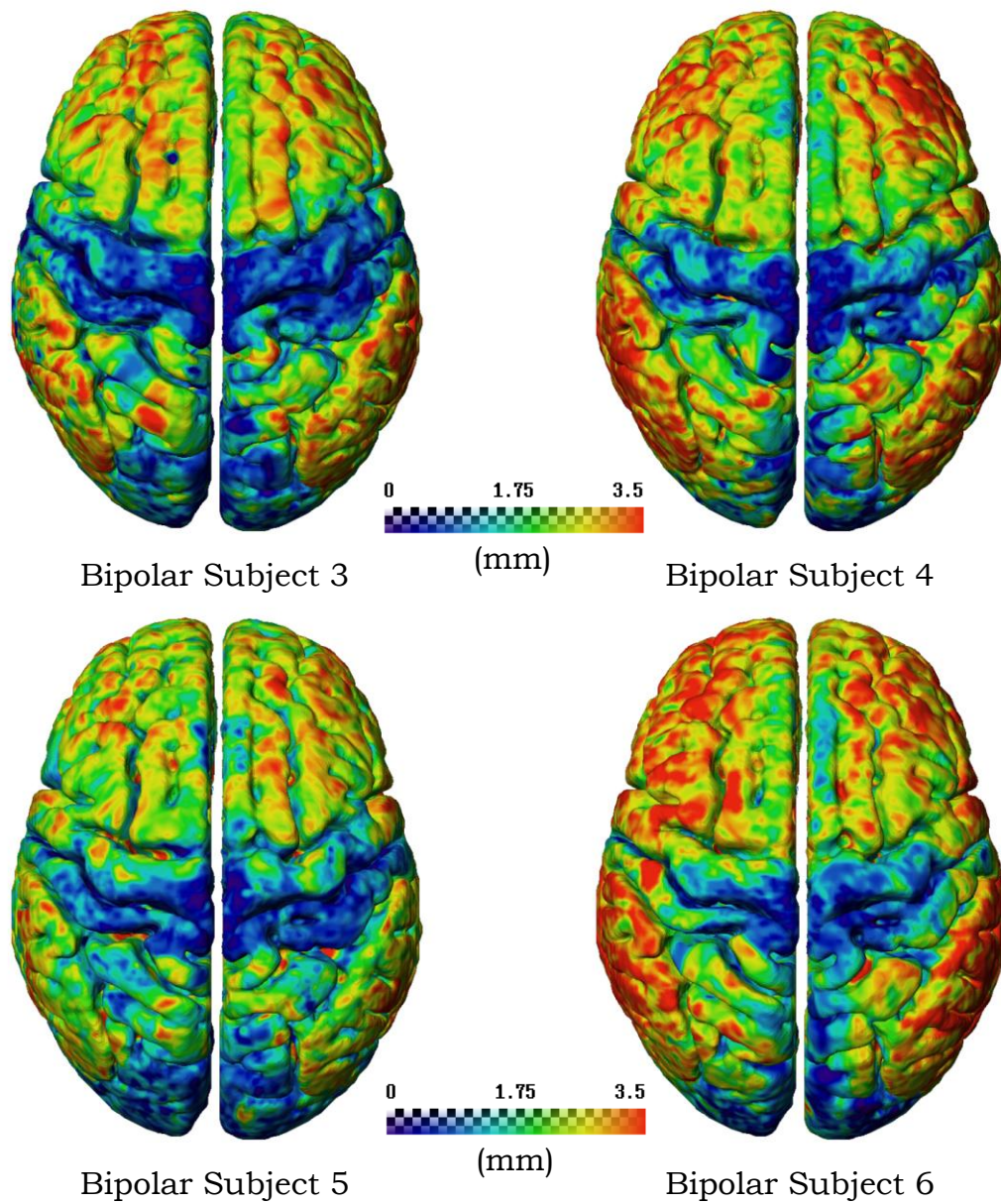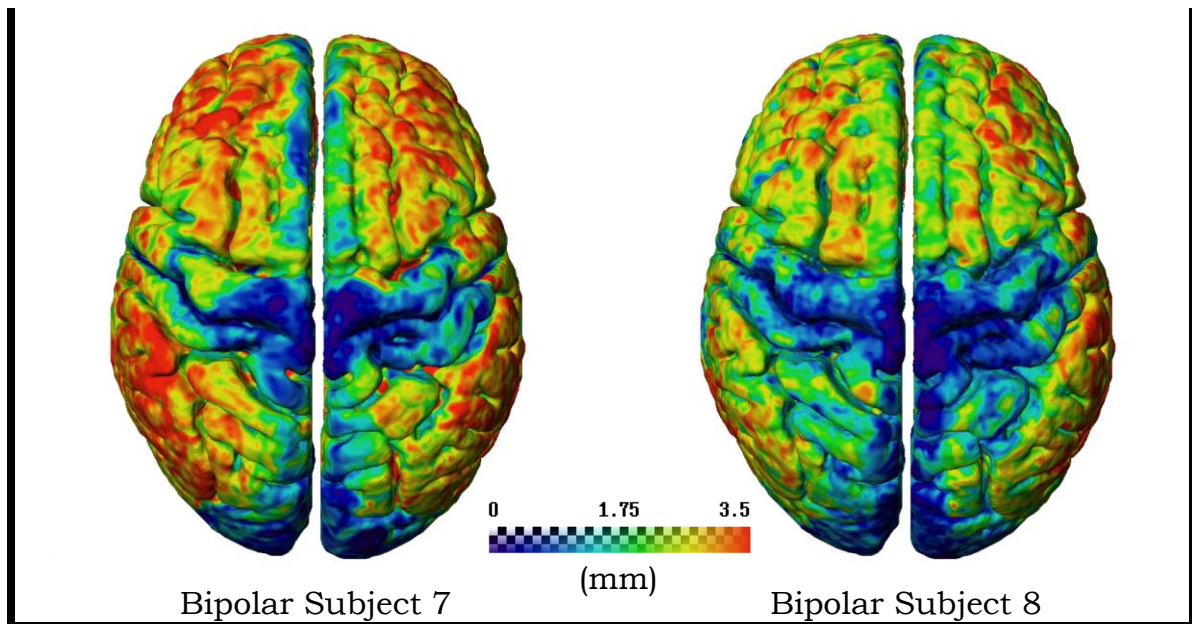
Figure 13 – GM-to-GMm of individuals in bipolar group.
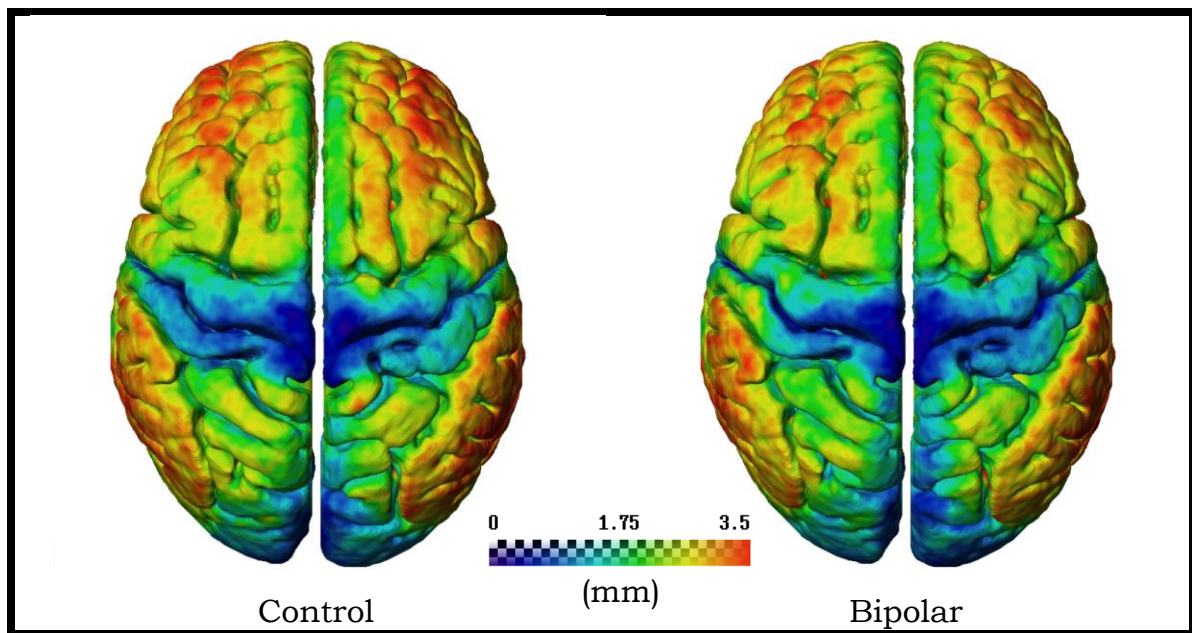
Figure 14 – Mean of GM-to-GMm.

Figure 15 – Standard deviation of GM-to-GMm.

Figure 16 – Coefficient of variation of GM-to-GMm.

Figure 17 – Mean difference and percent difference of GM-to-GMm.
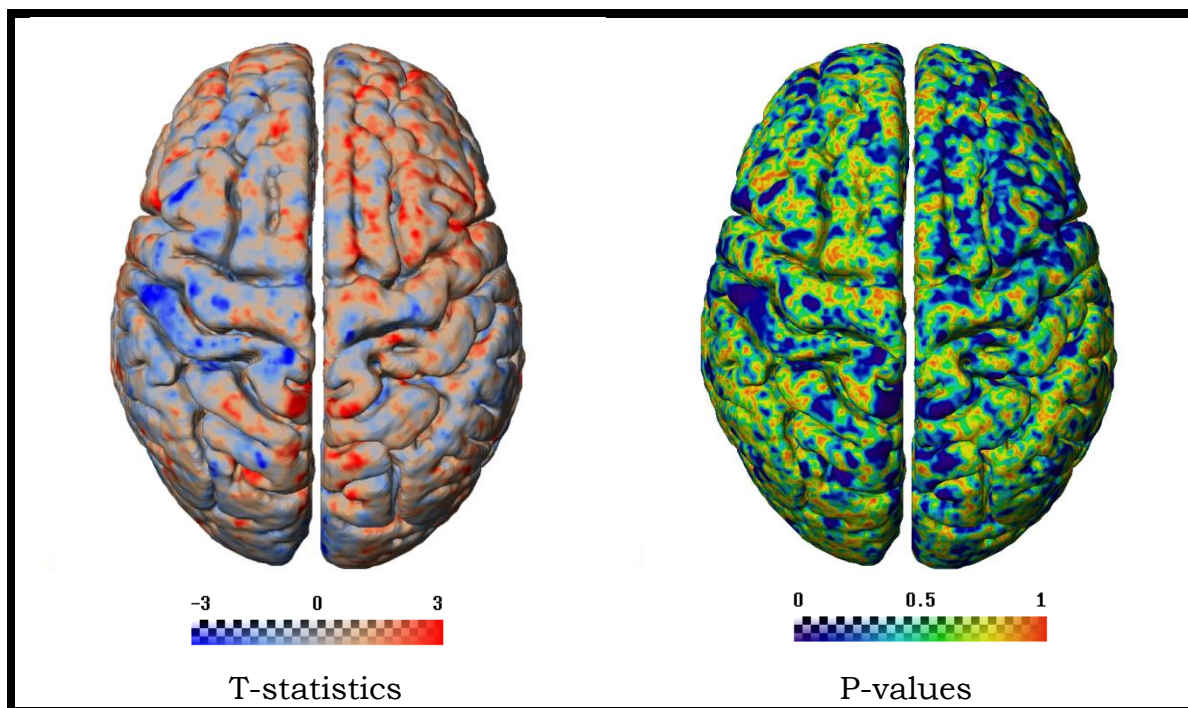
Figure 18 – T-statistics and p-values of GM-to-GMm.

p<0.05   p<0.001
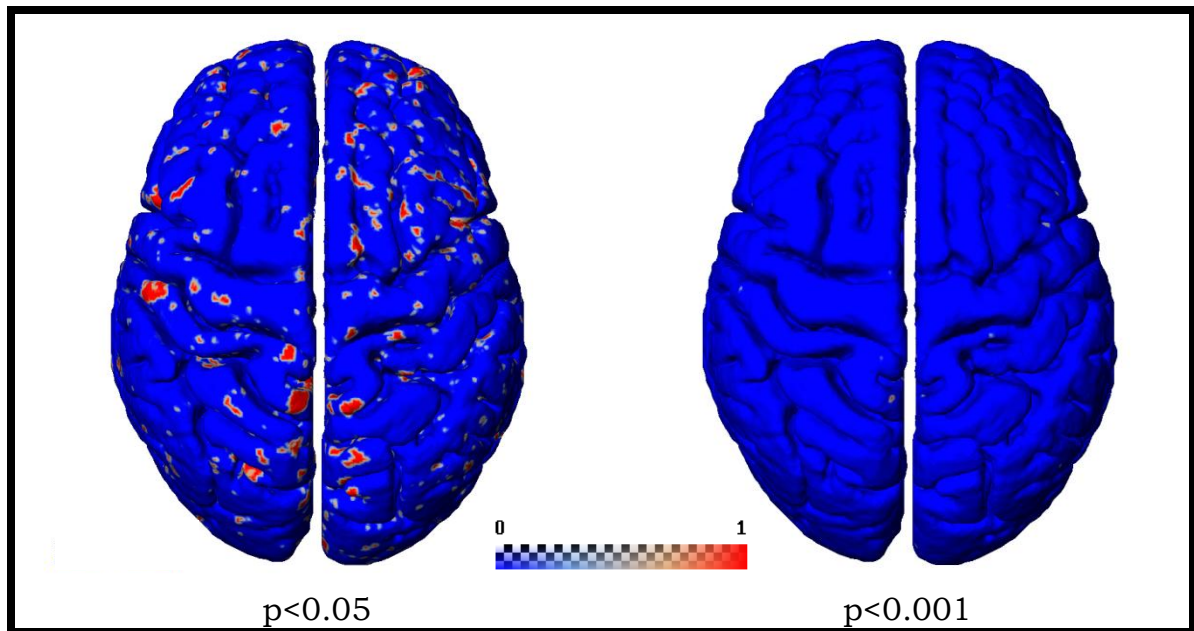
Figure 19 – Significances of GM-to-GMm.

3.3 Total Cortical Thickness

Figures 21 and 22 show the individual brains of control and bipolar subjects after registration, respectively. Figures 23, 24, and 25 show the means, standard deviations, and coefficients of variation, respectively. Figure 26 shows the difference of the means and the percent difference. Figure 27 shows the results of the t-test and the p-values. Figure 28 shows the areas of statistical significance.
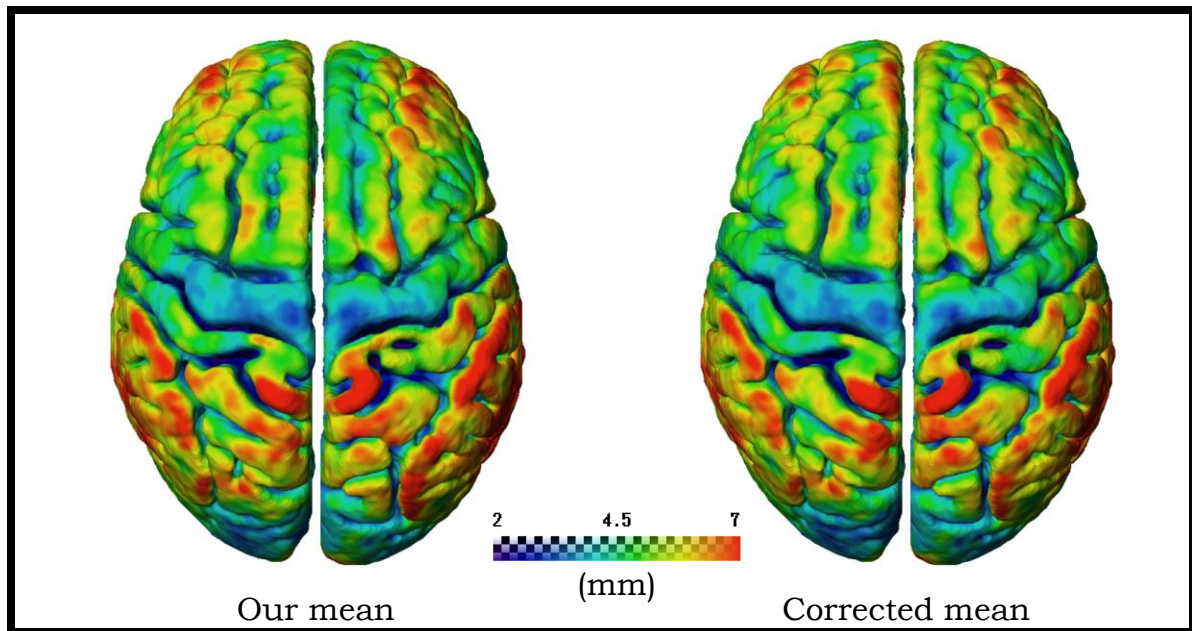
Figure 20 – GM-to-WM mean versus correct mean of controls.

Control Subject 3

(mm)

Control Subject 4

Control Subject 5

(mm)
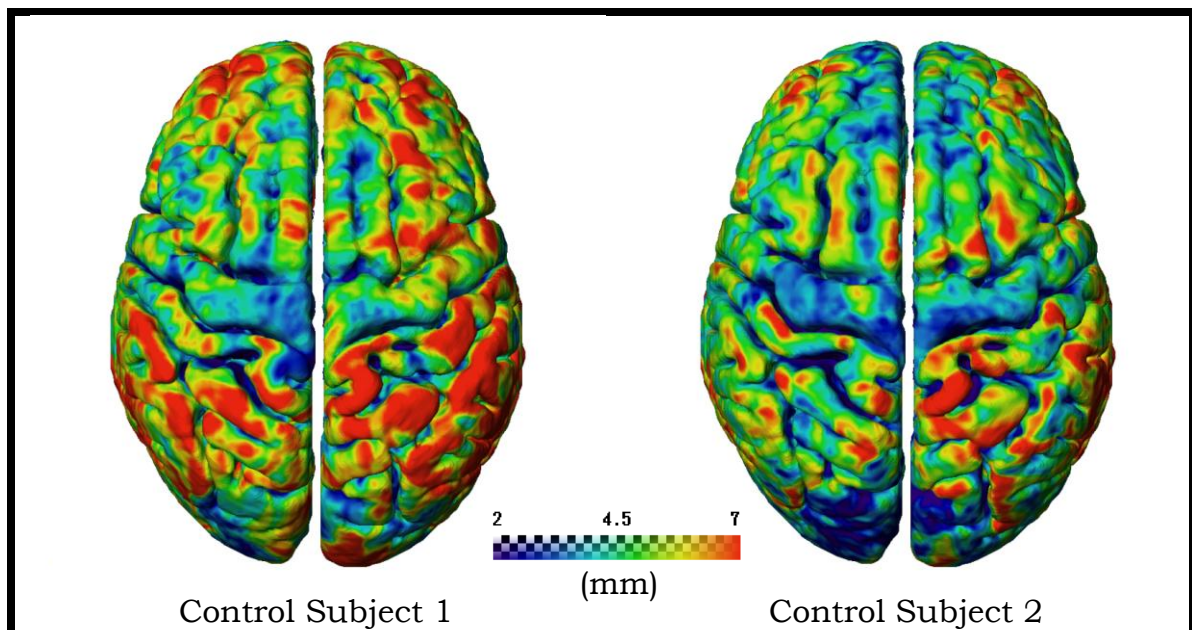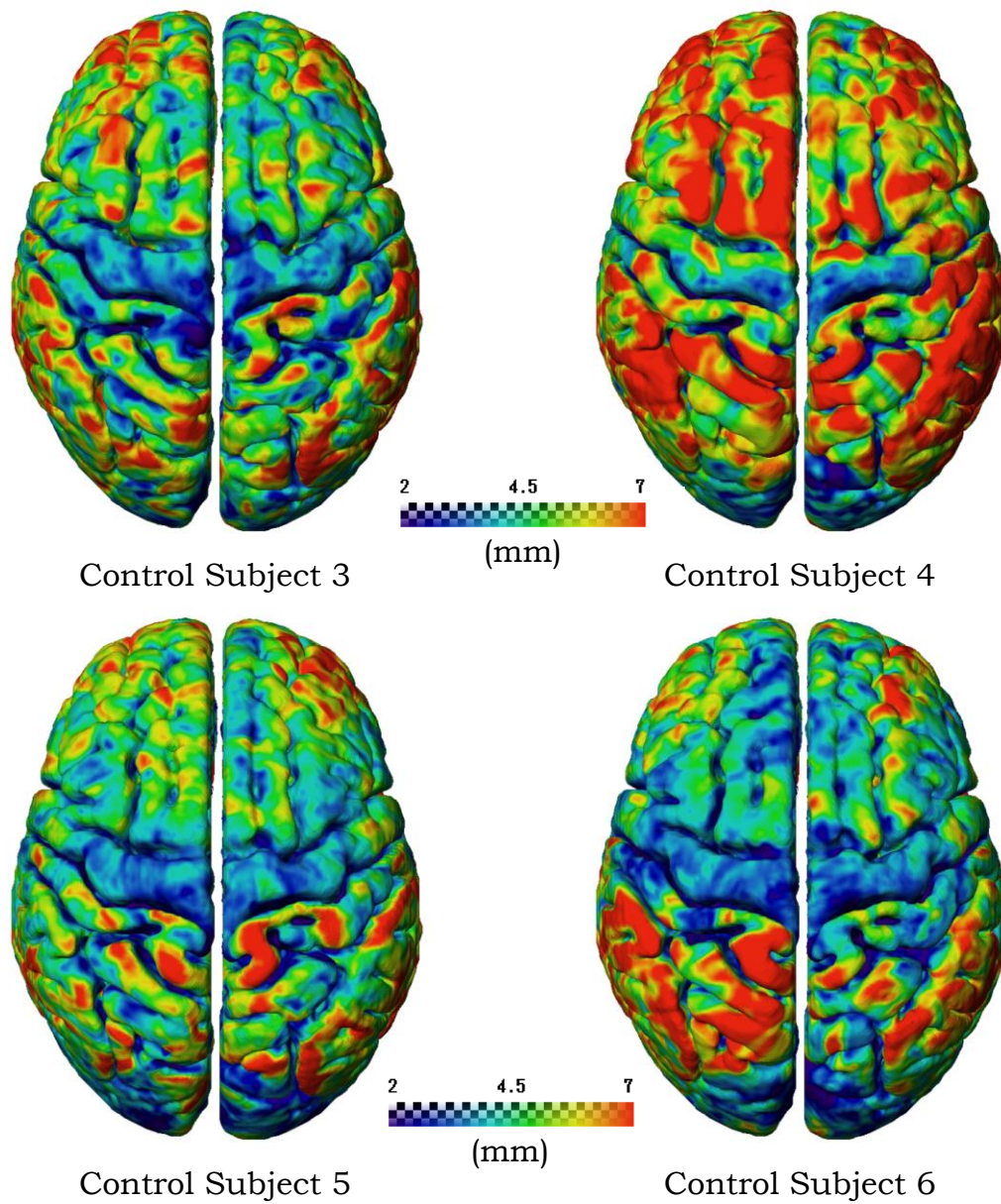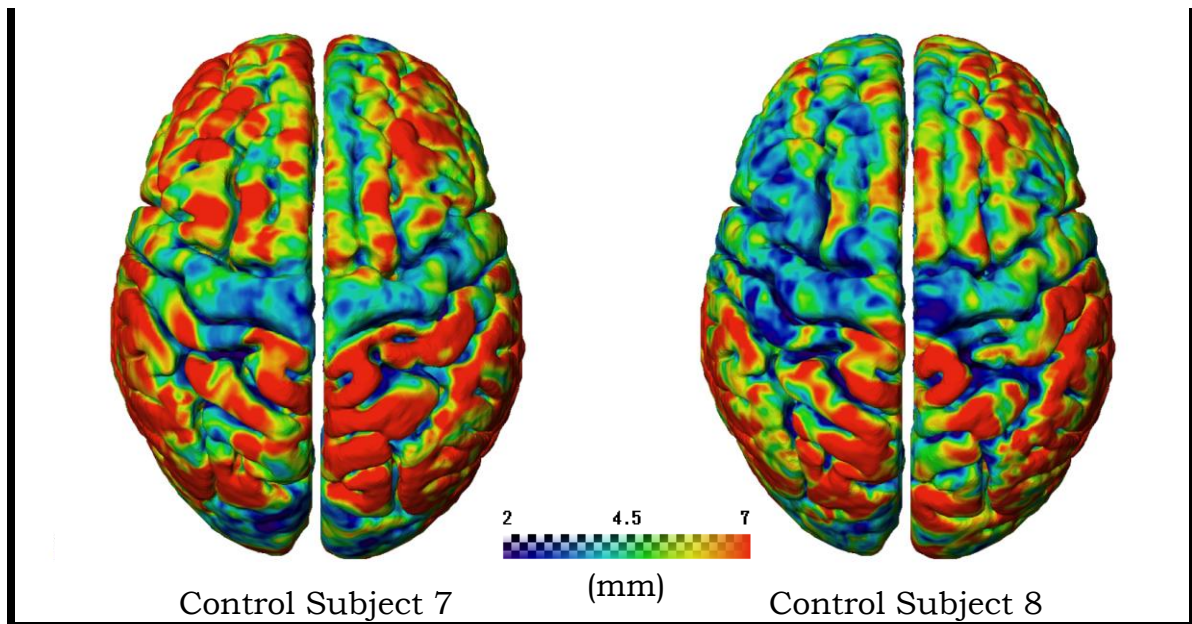
Control Subject 6

Figure 21 – GM-to-WM of individuals in control group.
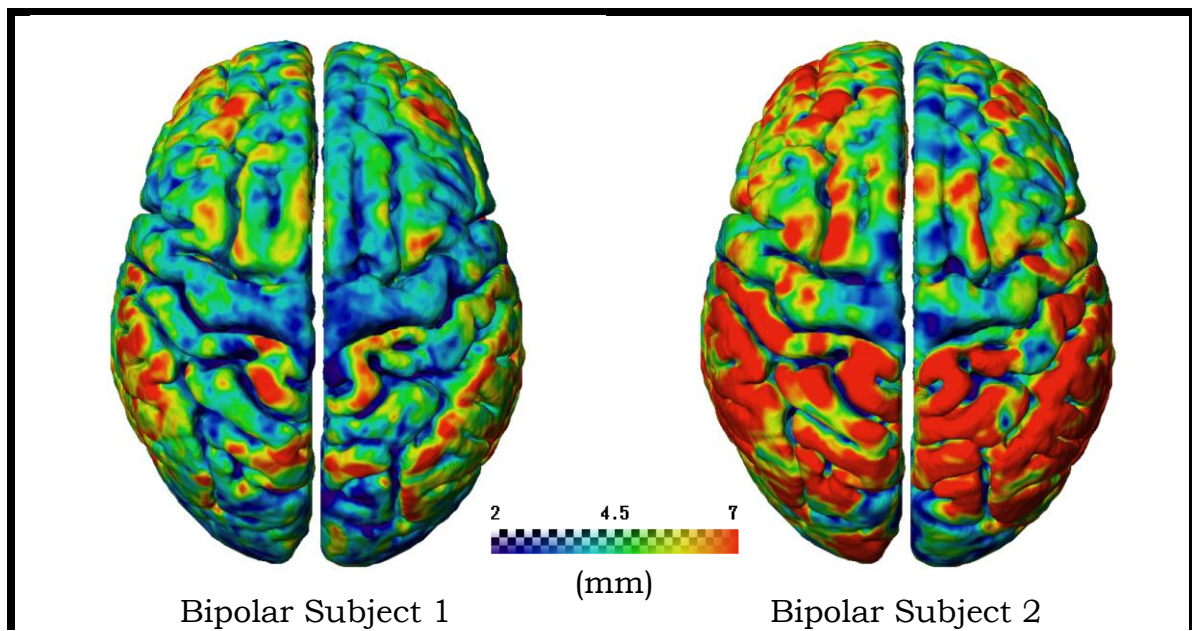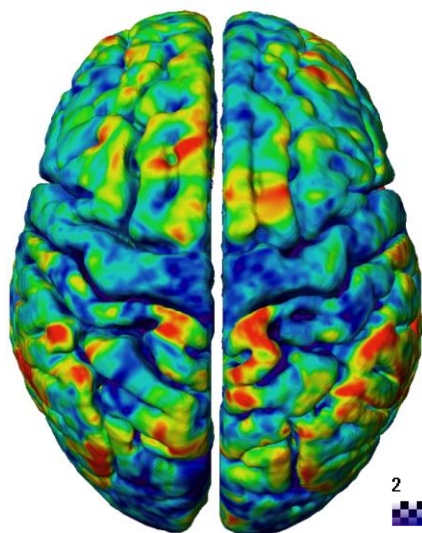
Bipolar Subject 3
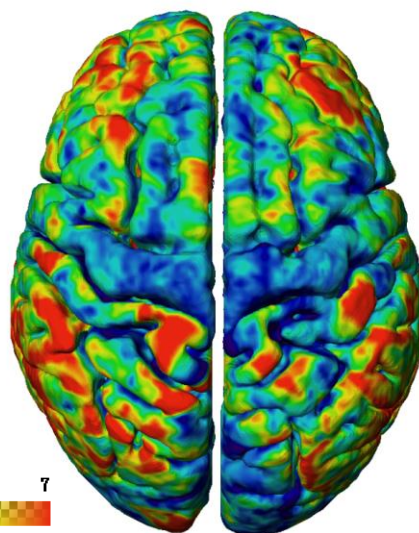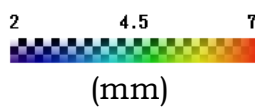
Bipolar Subject 4
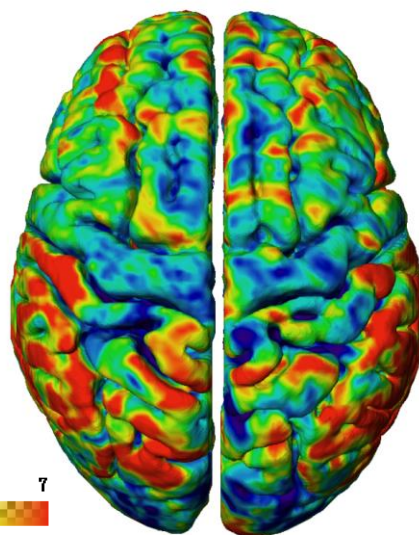
Bipolar Subject 5

Bipolar Subject 6
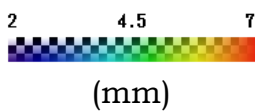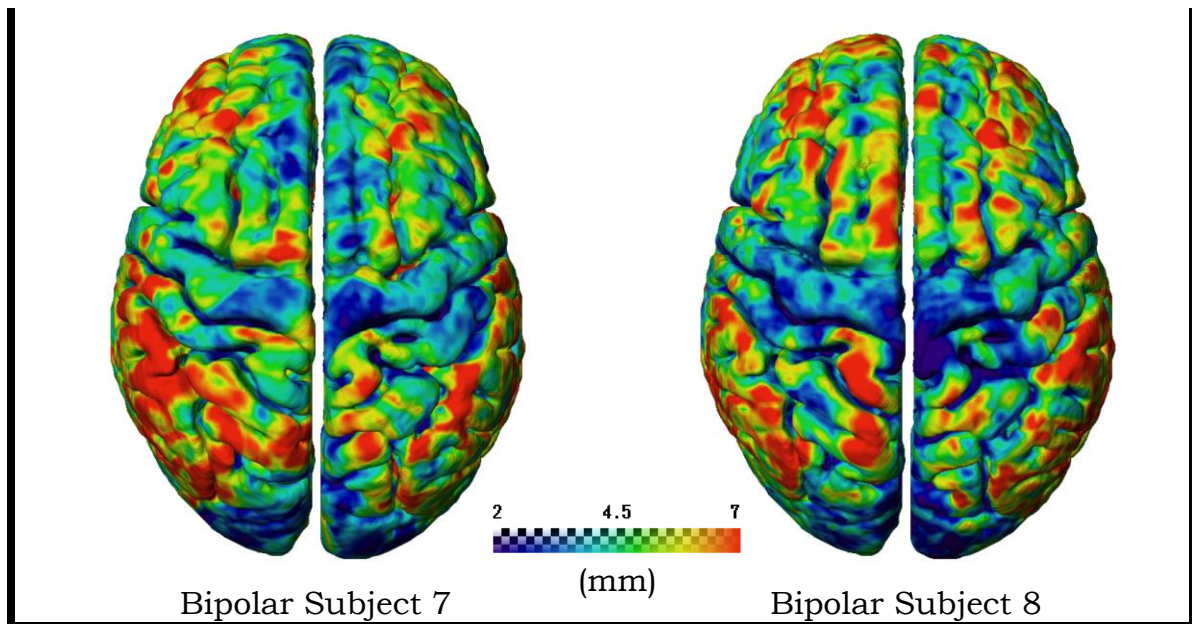
Figure 22 – GM-to-WM of individuals in bipolar group.
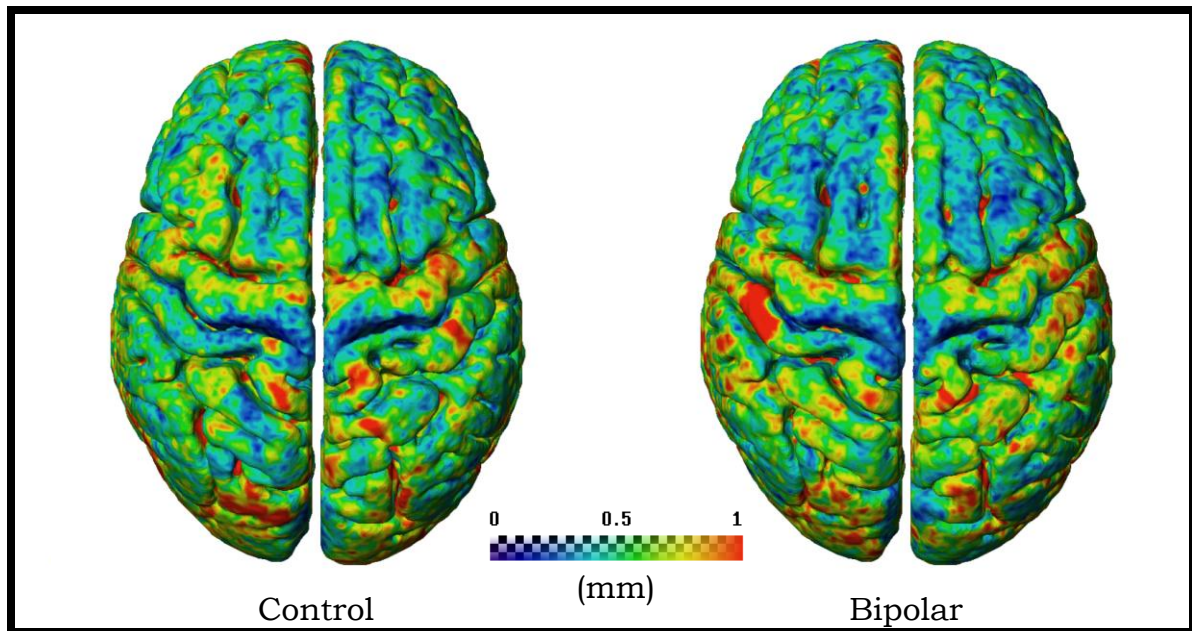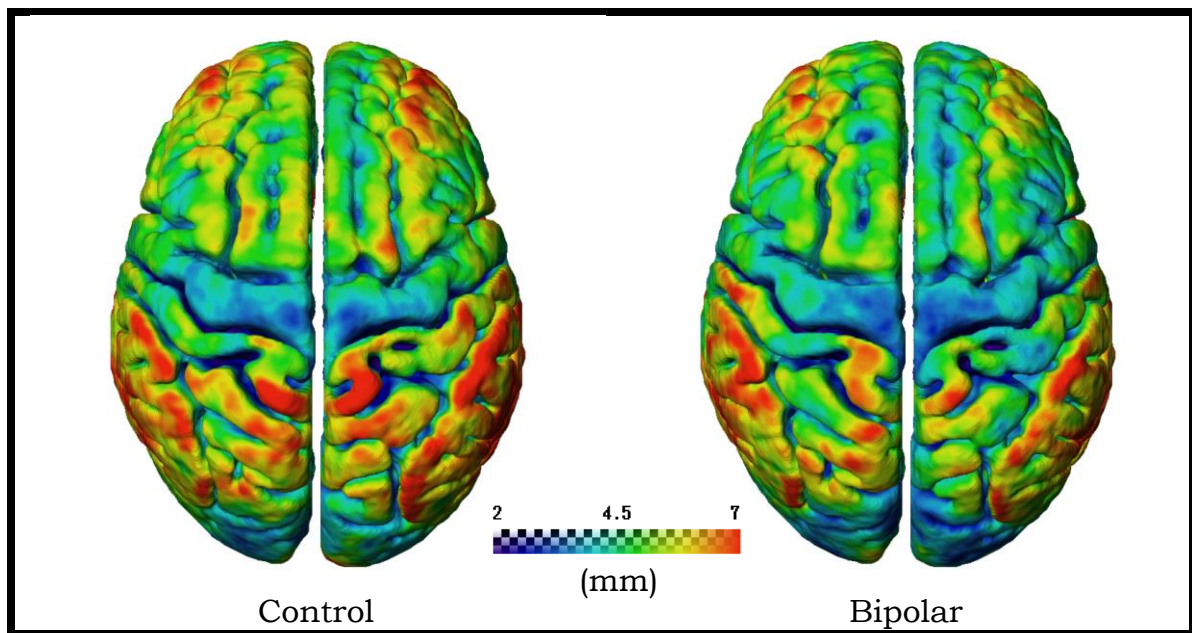

Figure 23 – Mean of GM-to-WM.
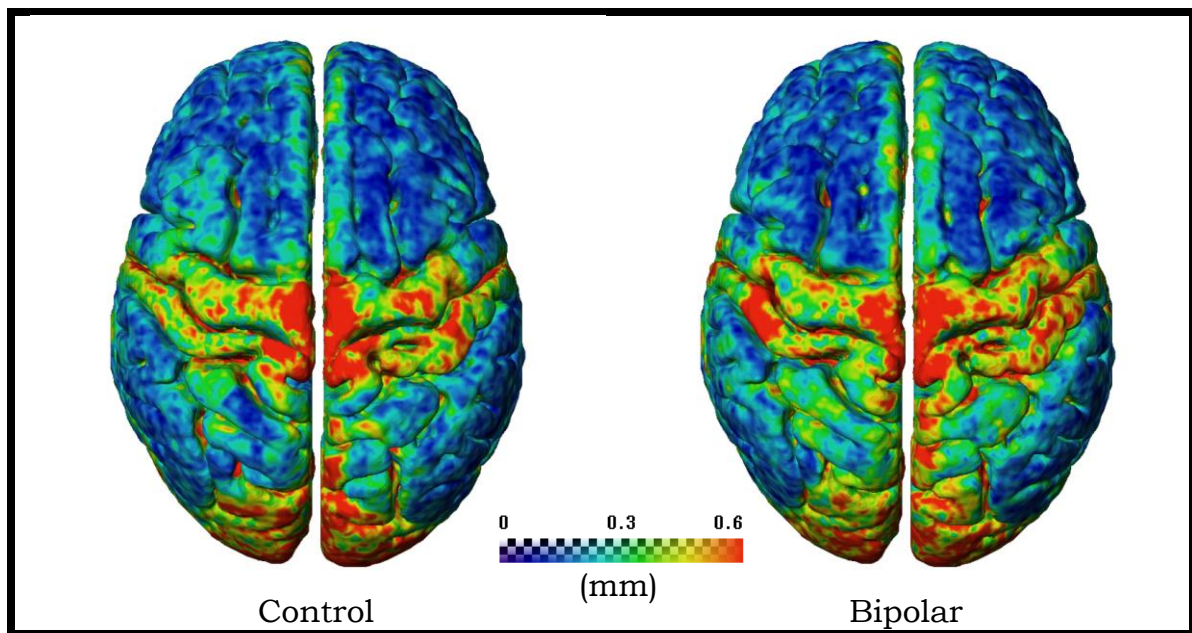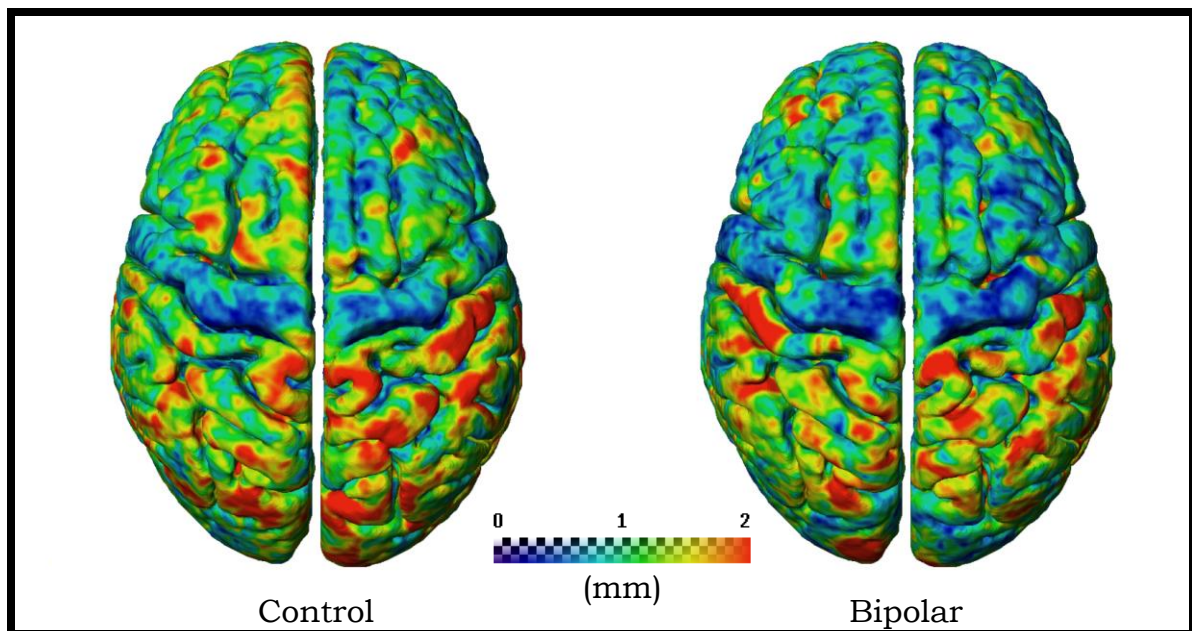
Figure 24 – Standard deviation of GM-to-WM.
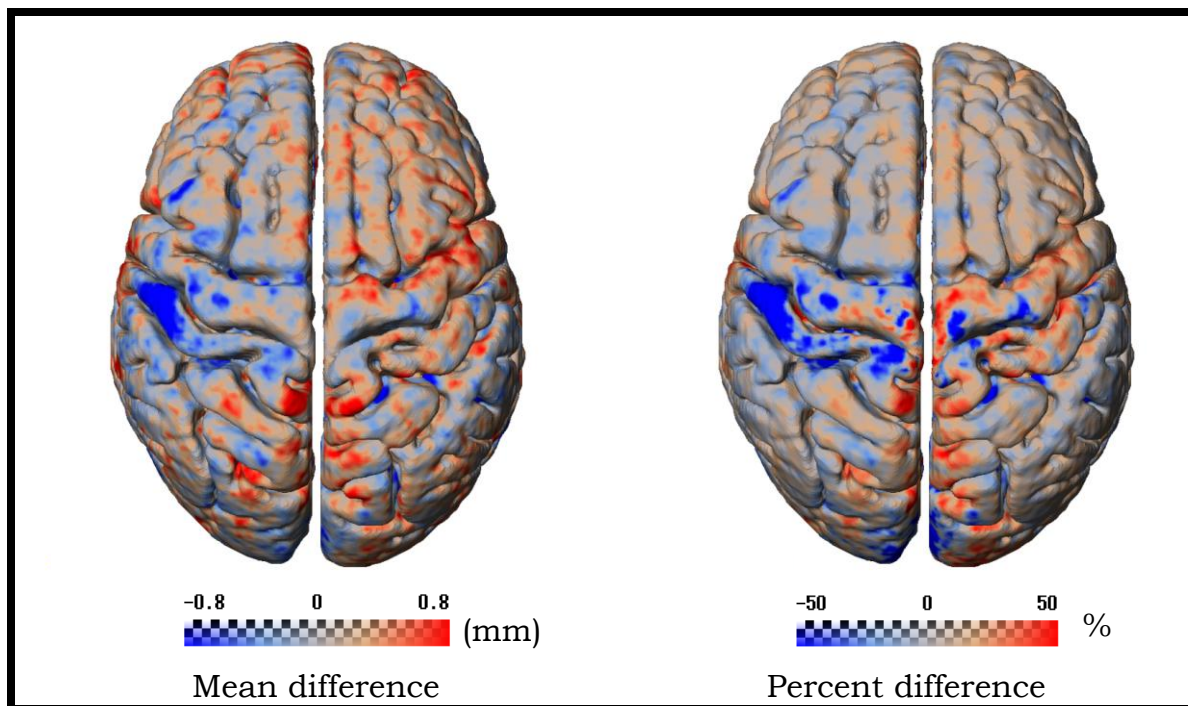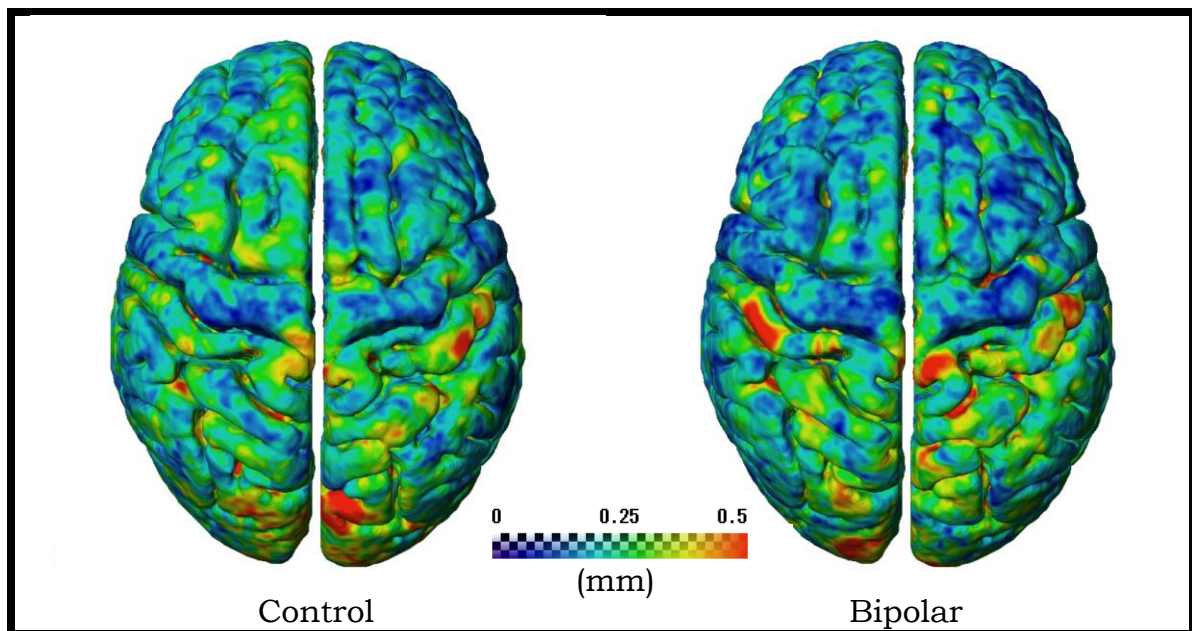

Figure 25 – Coefficient of variation of GM-to-WM.
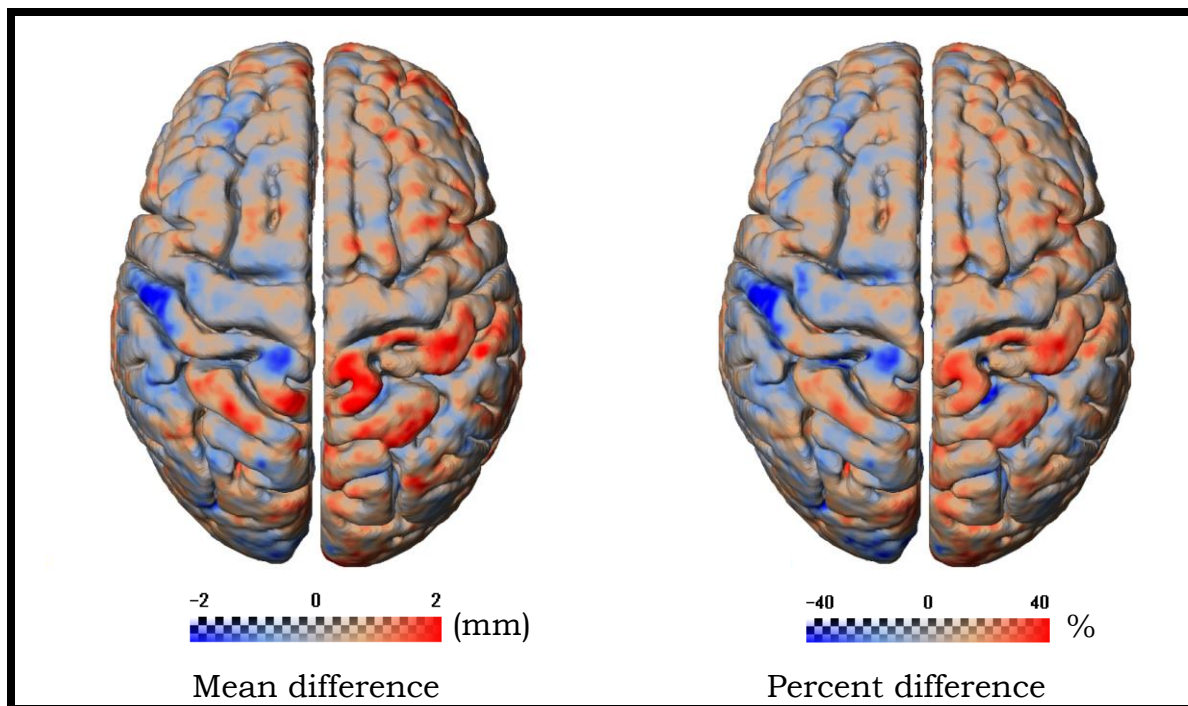
Figure 26 – Mean difference and percent difference of GM-to-WM.
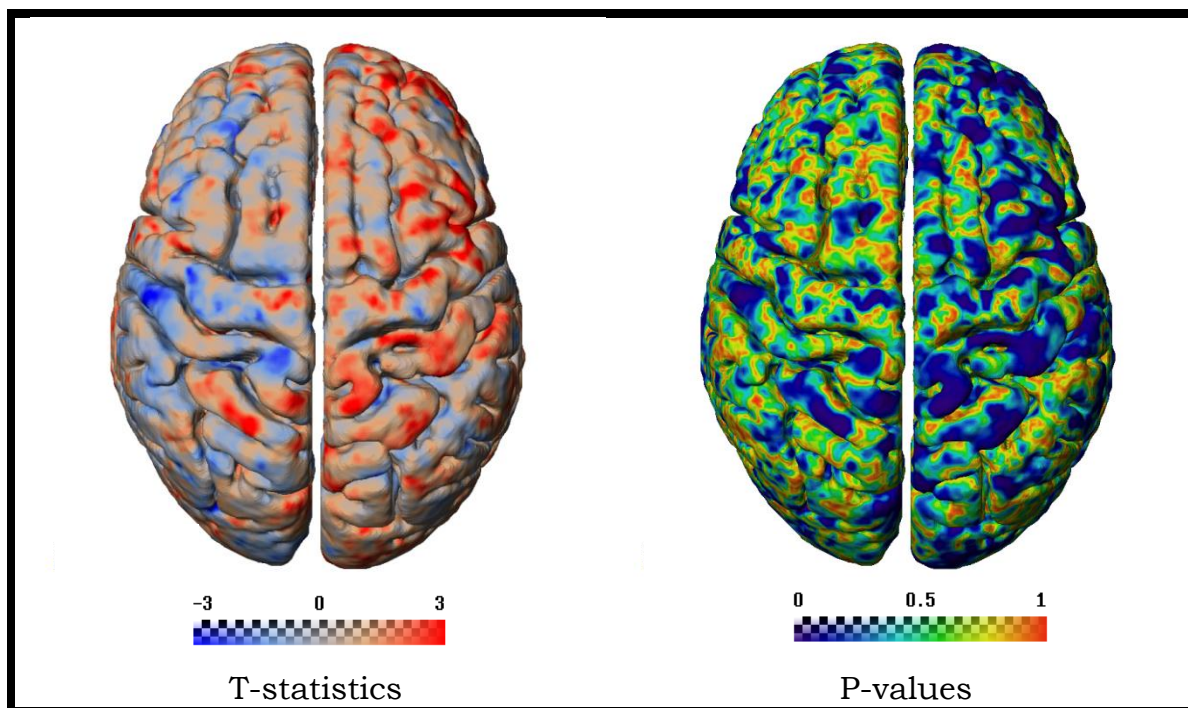

Figure 27 – T-statistics and p-values of GM-to-WM.
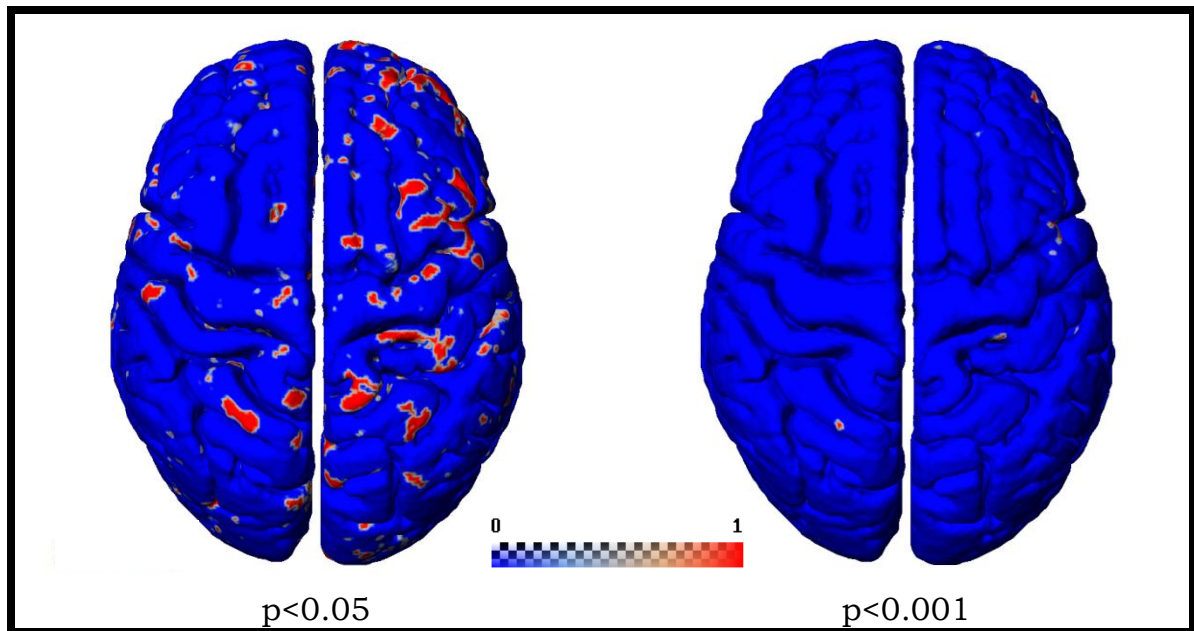
Figure 28 – Significances of GM-to-WM.

3.4 Results Summary

We observed notable differences between BP and control averages. Statistically, there were some significant differences for an uncorrected α of 0.05, but almost no difference for an α of 0.001, and no difference at all for a Bonferroni corrected α of 0.05. Although there are differences scattered all throughout the cortex, we see fairly consistent thinning in the left and right prefrontal areas, and less consistently noticeable differences in others parts of the cortex. It remains unclear whether either of the null hypotheses can be rejected, and further analysis is necessary.

CHAPTER 4 – DISCUSSION

This preliminary study shows promising results in the examination of intracortical myelin.

One downfall of our study is the low number of subjects (N=8 for each group). Less strict exclusion criteria may have allowed for a much higher number of subjects, which could then be filtered according to various cofactors for further study, such as age, IQ, or bipolar subtype. An analysis of covariance (ANCOVA) could be performed.

It may be interesting to study the effects of age on cortical thickness in BD versus control (Salat et al., 2004). It would also be worthwhile to examine if different medications have different effects on ICM, as suggested in schizophrenia studies (Bartzokis et al., 2009). Finally, it would be particularly meaningful to see if ICM differences are more prominent in bipolar I versus bipolar II, as sometimes appears to be the case with grey matter (Rimol et al., 2010). This could give some hints as to whether the severity of manic episodes plays a role in cortical thinning. It would also be of great interest to see if the duration of the illness or the number of manic/hypomanic episodes play a role, as suggested (Strakowski et al., 2004).

The analysis depends heavily on the assumption that the data in both groups is normally distributed. The t-test relies on this assumption and is no longer useful when it doesn't hold true. We also assumed that

the variances of both groups were equal, when they very well may not be. It is entirely possible that the data follows a different type of distribution. For example, perhaps there is a notable difference between bipolar I and II brains, causing a bimodal distribution. Perhaps there is a difference depending on the medication(s) used, the age, IQ, or other factors. With an N of 8, normality tests may not give meaningful results, but it is a good idea to apply them once the sample sizes increase.

Another good idea would be to apply a non-parametric test; one that does not make assumptions about the probability distributions of the data; or a test that models the distribution of the data, such as statistical bootstrapping using a Monte Carlo simulation (Adèr et al., 2008). Bootstrapping is highly recommended in situations where the theoretical distribution is unknown and the sample size is small (Adèr et al., 2008).

One thing that may improve the analysis is performing a surface-based spatial normalization instead of a volume normalization in the processing. Better results may also be obtained by spatially smoothing the data using a Gaussian kernel, but at the expense of the high resolution needed to identify the tissue boundaries. Finally, clustering the p-value results spatially would decrease the possibility of noise in the significance images, avoiding single voxels that indicate significance, for example.

In order to make the statistical analysis more robust, it's clear that the next step would be to divide the brain up into ROI's. It has also become clear that the data points of interest – the voxels on the pial surface of the brain – need to be separated from the rest of the data. This is not trivial and depends on the type of surface mapping used. Once these two steps are completed, the Bonferroni correction can be applied with fewer problems. Additionally, averages can be taken within each ROI and compared across ROI's. If desired, some of the more advanced techniques described earlier such as PCA, resampling, RFT, or FDR, can be applied. A power analysis can be performed to determine the minimum sample size needed for similar results to be significant.

Although the sample size is currently too small to be conclusive, the results obtained seem very promising. The concept of dividing the brain into three tissue types can be tested in any neuroimaging study where previously only two tissue types, GM and WM, have been examined. This gives rise to an enormous potential for new research.

These new methods of obtaining, processing, and analyzing anatomical brain data bring us one step closer to understanding the complex system that is the brain.

REFERENCES

1. Kandel, Eric R.; Schwartz, James H.; Jessell, Thomas M. (2000). Principles of Neural Science (Fourth Edition). United States of America: McGraw-Hill. p. 324. ISBN 0-8385-7701-6.

2. Nieuwenhuys, R. (2013). The myeloarchitectonic studies on the human cerebral cortex of the Vogt-Vogt school, and their significance for the interpretation of functional neuroimaging data. *Brain structure & function,218*(2), 303–52. doi:10.1007/s00429-012-0460-z

3. Bock, N., Kocharyan, A., Liu, J., & Silva, A. (2009). Visualizing the entire cortical myelination pattern in marmosets with magnetic resonance imaging. *Journal of neuroscience methods, 185*(1), 15–22. doi:10.1016/j.jneumeth.2009.08.022

4. Rosas, H., Liu, A., Hersch, S., Glessner, M., Ferrante, R., Salat, D., … Fischl, B. (2002). Regional and progressive thinning of the cortical ribbon in Huntington's disease. *Neurology, 58*(5), 695701. doi:10.1212/WNL.58.5.695

5. Sailer, M., Fischl, B., Salat, D., Tempelmann, C., Schönfeld, M., Busa, E., … Dale, A. (2003). Focal thinning of the cerebral cortex in multiple sclerosis.*Brain, 126*(8), 1734–1744. doi:10.1093/brain/awg175

6. Querbes, O., Aubry, F., Pariente, J., Lotterie, J.-A., Démonet, J.-F., Duret, V., … Initiative, A. (2009). Early diagnosis of Alzheimer's disease using cortical thickness: impact of cognitive reserve. *Brain : a journal of neurology, 132*(Pt 8), 2036–47. doi:10.1093/brain/awp105

7. Pereira, J., Ibarretxe-Bilbao, N., Marti, M.-J., Compta, Y., Junqué, C., Bargallo, N., & Tolosa, E. (2012). Assessment of cortical degeneration in patients with Parkinson's disease by voxel-based morphometry, cortical folding, and cortical thickness. *Human brain mapping, 33*(11), 2521–34. doi:10.1002/hbm.21378

8. Makris, N., Biederman, J., Valera, E., Bush, G., Kaiser, J., Kennedy, D., … Seidman, L. (2007). Cortical Thinning of the Attention and Executive Function Networks in Adults with Attention-

Deficit/Hyperactivity Disorder. *Cerebral Cortex, 17*(6), 1364–1375. doi:10.1093/cercor/bhl047

9. Narr, K., Bilder, R., Toga, A., Woods, R., Rex, D., Szeszko, P., … Thompson, P. (2005). Mapping Cortical Thickness and Gray Matter Concentration in First Episode Schizophrenia. *Cerebral Cortex, 15*(6), 708–719. doi:10.1093/cercor/bhh172

10. Truong, W., Minuzzi, L., Soares, C., Frey, B., Evans, A., MacQueen, G., & Hall, G. (2013). Changes in cortical thickness across the lifespan in major depressive disorder. *Psychiatry research, 214*(3), 204–11. doi:10.1016/j.pscychresns.2013.09.003

11. Lyoo, I. K., Sung, Y. H., Dager, S. R., Friedman, S. D., Lee, J.-Y. Y., Kim, S. J., … Renshaw, P. F. (2006). Regional cerebral cortical thinning in bipolar disorder.*Bipolar disorders, 8*(1), 65–74. doi:10.1111/j.1399-5618.2006.00284.x

12. Hutton, C., Draganski, B., Ashburner, J., & Weiskopf, N. (2009). A comparison between voxel-based cortical thickness and voxel-based morphometry in normal aging. *NeuroImage, 48*(2), 371–80. doi:10.1016/j.neuroimage.2009.06.043

13. Bartzokis, G., Lu, P., Stewart, S., Oluwadara, B., Lucas, A., Pantages, J., … Nuechterlein, K. (2009). In vivo evidence of differential impact of typical and atypical antipsychotics on intracortical myelin in adults with schizophrenia. *Schizophrenia research, 113*(2-3), 322–31. doi:10.1016/j.schres.2009.06.014

14. Strakowski, S., DelBello, M., & Adler, C. (2004). The functional neuroanatomy of bipolar disorder: a review of neuroimaging findings. *Molecular Psychiatry, 10*(1), 105–116. doi:10.1038/sj.mp.4001585

15. American Psychiatric Association. (2000). *Diagnostic and statistical manual of mental disorders* (4th ed., text rev.). doi:10.1176/appi.books.9780890423349.

16. McRobbie, Donald W. (2007). *MRI from picture to proton* (2nd ed.). Cambridge, UK ; New York: Cambridge University Press. ISBN 0-521-68384-X.

17. Callaghan, P. T. (1991). *Principles of nuclear magnetic resonance microscopy* (Vol. 3). Oxford: Clarendon Press. ISBN 0-19-853997-5.

18. Bock, N., Hashim, E., Janik, R., Konyer, N., Weiss, M., Stanisz, G., … Geyer, S. (2013). Optimizing T1-weighted imaging of cortical myelin content at 3.0 T.*NeuroImage*, *65*, 1–12. doi:10.1016/j.neuroimage.2012.09.051

19. Kapur, T., Grimson, W., III, W., & Kikinis, R. (1996). Segmentation of brain tissue from magnetic resonance images. *Medical Image Analysis*, *1*(2), 109127. doi:10.1016/S1361-8415(96)80008-9

20. Hashim, E., Bazin, PL., Zaharieva, N., Rowley, C., Bock, N. (Submitted 2014). Myelinated Cortical Thickness Measurements.

21. Frey, BN. (Submitted 2014). Cortical Myelin Content Mapping in Bipolar Disorder.

22. Jenkinson, M., Beckmann, C., Behrens, T., Woolrich, M., & Smith, S. (2012). FSL. *NeuroImage*, *62*(2), 782–90. doi:10.1016/j.neuroimage.2011.09.015

23. Carass, A., Cuzzocreo, J., Wheeler, M., Bazin, P.-L., Resnick, S., & Prince, J. (2011). Simple paradigm for extra-cerebral tissue removal: algorithm and analysis.*NeuroImage*, *56*(4), 1982–92. doi:10.1016/j.neuroimage.2011.03.045

24. Bogovic, J., Prince, J., & Bazin, P.-L. (2012). A multiple object geometric deformable model for image segmentation. *Computer Vision and Image Understanding*. doi:10.1016/j.cviu.2012.10.006

25. Landman, B., Bogovic, J., Carass, A., Chen, M., Roy, S., Shiee, N., … Prince, J. (2013). System for integrated neuroimaging analysis and processing of structure.*Neuroinformatics*, *11*(1), 91–103. doi:10.1007/s12021-012-9159-9

26. Pham, DL. (2001). Robust fuzzy segmentation of magnetic resonance images. doi:10.1109/CBMS.2001.941709

27. Sethian, J. A. (1999). *Level set methods and fast marching methods: evolving interfaces in computational geometry, fluid mechanics, computer vision, and materials science* (Vol. 3). Cambridge university press.

28. Fonov, V., Evans, A., Botteron, K., Almli, C., McKinstry, R., Collins, D., & Group, B. (2011). Unbiased average age-appropriate atlases for pediatric studies. *NeuroImage, 54*(1), 313–27. doi:10.1016/j.neuroimage.2010.07.033

29. Fonov, V. S., Evans, A. C., McKinstry, R. C., Almli, C. R., & Collins, D. L. (2009). Unbiased nonlinear average age-appropriate brain templates from birth to adulthood. *NeuroImage, 47*, S102. doi:10.1016/S1053-8119(09)70884-5

30. Lindquist, M. (2008). The Statistical Analysis of fMRI Data. *arXiv, 23*(4), 439464. doi:10.1214/09-STS282

31. Genovese, C., Lazar, N., & Nichols, T. (2002). Thresholding of Statistical Maps in Functional Neuroimaging Using the False Discovery Rate.*NeuroImage, 15*(4), 870878. doi:10.1006/nimg.2001.1037

32. Thompson, P., Vidal, C., Giedd, J., Gochman, P., Blumenthal, J., Nicolson, R., ... Rapoport, J. (2001). Mapping adolescent brain change reveals dynamic wave of accelerated gray matter loss in very early-onset schizophrenia. *Proceedings of the National Academy of Sciences*, *98*(20), 11650–11655. doi:10.1073/pnas.201243998

33. Sowell, E., Peterson, B., Thompson, P., Welcome, S., Henkenius, A., & Toga, A. (2003). Mapping cortical change across the human life span. *Nature Neuroscience*,*6*(3), 309315. doi:10.1038/nn1008

34. Schwartzman, A., Dougherty, R., Lee, J., Ghahremani, D., & Taylor, J. (2009). Empirical null and false discovery rate analysis in neuroimaging. *NeuroImage*,*44*(1), 71–82. doi:10.1016/j.neuroimage.2008.04.182

35. Shaw, P., Lerch, J., Greenstein, D., Sharp, W., Clasen, L., Evans, A., ... Rapoport, J. (2006). Longitudinal Mapping of Cortical Thickness and Clinical Outcome in Children and Adolescents With Attention-Deficit/Hyperactivity Disorder. *Archives of General Psychiatry, 63*(5), 540–549. doi:10.1001/archpsyc.63.5.540

36. Rimol, L., Hartberg, C., Nesvåg, R., Fennema-Notestine, C., Hagler, D., Pung, C., ... Agartz, I. (2010). Cortical thickness and

subcortical volumes in schizophrenia and bipolar disorder. *Biological psychiatry*,*68*(1), 41–50. doi:10.1016/j.biopsych.2010.03.036

37. Thompson, P., Dutton, R., Hayashi, K., Toga, A., Lopez, O., Aizenstein, H., & Becker, J. (2005). Thinning of the cerebral cortex visualized in HIV/AIDS reflects CD4+ T lymphocyte decline.*Proceedings of the National Academy of Sciences of the United States of America, 102*(43), 15647. doi:10.1073/pnas.0502548102

38. Foland-Ross, L. C., Thompson, P. M., Sugar, C. A., Madsen, S. K., Shen, J. K., Penfold, C., … Altshuler, L. L. (2011). Investigation of cortical thickness abnormalities in lithium-free adults with bipolar I disorder using cortical pattern matching. *The American journal of psychiatry, 168*(5), 530–9. doi:10.1176/appi.ajp.2010.10060896

39. Rosas, H., Liu, A., Hersch, S., Glessner, M., Ferrante, R., Salat, D., … Fischl, B. (2002). Regional and progressive thinning of the cortical ribbon in Huntington's disease. *Neurology, 58*(5), 695701. doi:10.1212/WNL.58.5.695

40. Salat, D., Buckner, R., Snyder, A., Greve, D., Desikan, R., Busa, E., … Fischl, B. (2004). Thinning of the Cerebral Cortex in Aging. *Cerebral Cortex, 14*(7), 721–730. doi:10.1093/cercor/bhh032

41. Adèr, H. J., Mellenbergh, G. J. (2008). *Advising on research methods: A consultant's companion*. Johannes van Kessel Publishing. ISBN 978-90-79418-01-5.